Article

Spatio – Temporal Characteristics of the Aftershocks Sequences that followed the Strong Earthquakes in Ionian Islands, Greece

Alexandra Moshou[1]*, George Drakatos[1], Vassilios Moussas[2], Panagiotis Argyrakis[1,3,5], Antonios Konstantaras[4], Anna Christina Daverona[3], Dimos Pantazis[3] and Nikos C. Sagias[5]

[1] Institute of Geodynamics, National Observatory of Athens; amoshou@noa.gr, g.drakat@noa.gr, pargyrak@noa.gr
[2] Dept. of Civil Engineering, University of West Attica; vmouss@uniwa.gr
[3] Dept. of Surveying and Geoinformatics Engineers, Faculty of Engineering, University of West Attica; adaverona@uniwa.gr, dnpantazis@uniwa.gr
[4] Dept. of Electronic Engineering, Hellenic Mediterranean University; akonstantaras@hmu.gr
[5] Dept. Informatics and Telecommunications, University of Peloponnese, Tripoli; nsagias@uop.gr

* Correspondence: amoshou@noa.gr; Tel.: +30-2103490152

Abstract: During the period January 2014 – October 2018, four strong earthquakes occurred in the Ionian Sea, Greece. A rich aftershock sequence followed each event of them. More analytically, according to the manual solutions of National Observatory of Athens, the first event (K1), occurred on 26 January 2014 in Kefallinia Island with magnitude M_L = 5.8, which was followed by another in the same region (K2) on 3 February 2014 with magnitude M_L = 5.7. The third event occurred on 17 November 2015, M_L = 6.0 in Lefkas Island (L1) and the last on 25 October 2018, M_L = 6.6 in Zande Island (Z1). The first three of these earthquakes caused moderate structural damages mainly in houses and produced particular unrest to the local population. This work presents first the calculation of the source parameters of the strong events as well as for all earthquakes with magnitude M_L > 4.0, using the methodology of the Moment tensor inversion and secondary data from permanent GPS stations were analyzed to confirm the findings from seismological data and to investigate the displacement due to the earthquakes.

Keywords: earthquake; source observations; body wave modeling; seismicity; ionian sea; gnss; machine learning; neural network

1. Introduction

In this work, a detailed seismological analysis of the Ionian Islands is performed. This area is characterized by continuous seismic activity and frequent occurrence of large earthquakes. The tectonic structure of the islands of Kefallinia and Ithaca is a result of the effect of compressive stresses in which periods of tensile stresses are inserted [1].

In the light of kinematics, the faults of Kefallinia are classified into the following categories [2]:

- reverse faults in the area of Argostoli
- reverse faults with either horizontal or vertical slip component (area of Ainos - Ag. Efthymia)
- horizontal slip faults - Argostoli, Paliki and SE Kefallinia area

The most characteristic tectonic structure of the study area is the clockwise fault of Kefallinia (Cephalonia Transform Fault Zone), which consists of the part of Lefkas to the north with direction NW - NN and the part of Cephalonia to the south with direction NW [3]. The existence of this transformation fault had been suggested by both depth studies [4], [5], [6] and geological mapping [7], [8], [9].

Preprints (www.preprints.org) | NOT PEER-REVIEWED | Posted: 4 September 2020 doi:10.20944/preprints202009.0080.v1

The first seismological indications for horizontal sliding movements in the study area were developed in the 1980s based on epicenters [10] and focal mechanisms of strong earthquakes and aftershocks of 17/01/1983 (M = 7.0) and 23/03/1983 (M = 6.2), [11], [12]. Further study by many scientists confirmed the effect of the horizontal slip fault in the area using synthetic waveform modeling [13], with micro-seismic studies [14] and geodetic measurements [15], [16]. The results from the micro-seismic [14], [17] and geodetic measurements [15], [16], led to the conclusion that this regime extends to the north in the area of Lefkas. Recent studies based on precise epicenters and genesis mechanisms confirm the existence of this seismically active fault of Kefallinia that runs parallel to the west coast of Lefkas [3]. These two parts of the fault, together with other smaller faults in the Ionian area, constitute the transformation brigade of Kefallinia and connect the fractured zone along the Hellenic arc in the South with that along with northern Greece and Western Albania.

The partner large seismotectonic structure that controls the seismicity of the wider area is the subsidence zone of the Greek arc section in the Ionian Sea area below Kefallinia that creates a complex seismotectonic structure [18].

The main objective of this paper is to study both the main events characteristics as well as their aftershocks' that occurred in the broader area of central Ionian Sea, Greece.

The statistical processing of aftershocks sequences is a useful key tool for understanding the focal mechanisms of the earthquake process. Changes in the rate of seismicity during seismic sequences indicate precursors to the generation of a strong earthquake during the sequence [19], [20], [21]. In this context, the present study examines the changes in the rate of seismicity during three seismic sequences, that of the Kefallinia earthquake (2014 – K1,2), the second of the Lefkas earthquake (2017 – L1) and the third the Zande earthquake (2018 – Z1).

Detailed Seismological data of these events were used in all the three main aspects of this work: The first and major part focuses on the extensional focal mechanisms of the main event and the comparison with those calculated from other institutions. In the second part, using GPS data and calculations of the GPS time series, the coseismic deformation is estimated. Finally, in the third part, a machine learning approach is used in order to define the major areas from where the events originate.

Table 1, presents the fault plane solutions of the major earthquakes that occurred in the study area (central Ionian Sea region) from 1959 – 2014. As can be seen, the focal mechanisms that had been calculated in the region of Kefallinia and those in the region of Lefkas fully agree with the seismotectonic setting of the broader area. More specifically, the activation of a dextral strike-slip fault is observed in Lefkas – Kefallinia area. In the South part of the Zande Island, the activation of a thrust fault is indicated.

Table 1: Moment tensor solutions from various sources determined for the events that occurred between 1953 and 2014 for the study area.

Date	Time	Lat	Lon	Depth	Mag	Strike	Dip	Rake	Region
15/11/1959	17:08:40	37.83	20.56	13	6.6	134	7	-90	Zande
16/12/1963	13:47:56	37.10	20.90	6	5.6	6	291	7	Zande
28/03/1968	7:39:00	37.80	20.90	6	5.9	120	71	64	Zande
8/7/1969	8:09:13	37.50	20.31	10	5.4	346	13	108	Zande
17/09/1972	14:07:16	38.28	20.34	8	5.6	39	61	-173	Kefallinia
4/11/1973	15:52:12	38.89	20.44	23	5.8	324	50	81	Lefkas
11/5/1976	16:59:48	37.56	20.35	13	6	323	13	90	Zande
12/6/1976	0:59:00	37.50	20.60	8	6	115	70	90	Zande
28/06/1981	17:20:23	37.81	20.06	14	6	15	76	180	Zande
17/01/1983	12:41:31	38.03	20.23	11	6	48	56	167	Kefallinia
19/01/1983	0:02:14	38.20	20.30	9	6	41	49	171	Kefallinia
31/01/1983	15:27:01	38.18	20.39	12	6	41	82	-177	Kefallinia

Preprints (www.preprints.org) | NOT PEER-REVIEWED | Posted: 4 September 2020 doi:10.20944/preprints202009.0080.v1

23/03/1983	23:51:07	38.29	20.26	7	6	30	70	176	Kefallinia
24/03/1983	4:17:31	38.09	20.29	18	6	62	70	172	Kefallinia
14/05/1983	23:13:48	38.44	20.33	13	6	36	86	167	Kefallinia
7/9/1985	10:20:50	37.50	21.20	29	5	24	57	168	Zande
27/02/1987	23:34:54	38.42	20.36	13	6	26	61	168	Kefallinia
18/05/1988	5:17:42	38.36	20.42	23	5	45	70	163	Kefallinia
16/10/1988	12:34:13	37.95	20.90	29	6	301	76	-3	Zande
20/08/1989	18:32:31	37.26	21.14	22	6	193	74	-174	Zande
24/08/1989	2:13:14	37.94	20.14	16	5	36	46	142	Zande
23/01/1992	4:24:19	38.40	20.57	9	6	345	19	68	Kefallinia
16/04/1994	23:09:34	37.36	20.63	22	6	124	76	90	Zande

2. Data and Methodology

2.1 Seismological Data

In this section, the seismological data collected and used for the analysis are presented. The significant seismic activity in the area of the central Ionian Islands is shown in Figure 1, where the epicenters of strong events (denoted by green, red and blue stars), as well as of the moderate earthquakes (denote by cycles colored respectively with the depth) are presented. The epicenter coordinates were adopted from the earthquake catalogues of the website of the National Observatory of Athens, https://bbnet.gein.noa.gr/HL/databases/database by selecting the study area and the time interval.

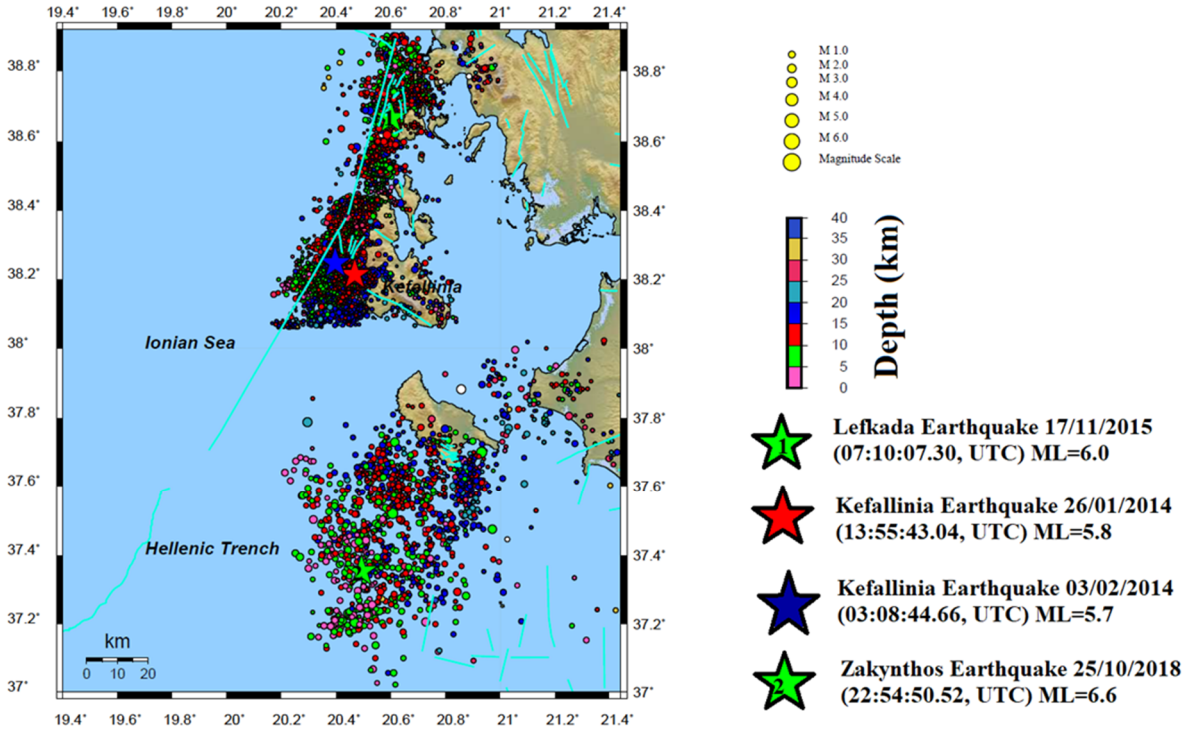

Figure 1: Epicenters of the main events as well as of the recorded aftershock sequence in Ionian Islands, (2014 – 2019). Red, green and blue stars indicate with respect to the depth the strong events for each seismic sequence, L1, K1,2 and Z1.

Preprints (www.preprints.org) | NOT PEER-REVIEWED | Posted: 4 September 2020 doi:10.20944/preprints202009.0080.v1

2.1.1 Fault Plane Solutions

In this section, the Moment Tensor Solutions for the strong events, as well as for all the moderate earthquakes from each aftershock sequence, were calculated and presented. For this purpose, seismological broadband data from the Hellenic Unified Seismological Network (HUSN) was collected, analyzed and used to determine the fault plane solution, the Moment Magnitude (Mw) and the Depth (d) of the strongest earthquakes of the K1,2, L1 and Z1 sequence.

For this purpose, a methodology based on a moment tensor inversion was used, as analytically described in [22] using the software of Ammon [23]. This method calculates synthetic seismograms directly compared with the observed ones for a given velocity structure. The reflectivity method of Kennett [24] as implemented by Randall [23] was applied to determine the Green Functions. Initially, Green's functions for different depths were calculated by the analyst. Initial inversions were performed at a depth interval of 5 km followed by a finer one every 1–2 km around the depth that exhibited the lowest misfit.

Regional data of five broadband stations, at different azimuth coverage and epicentral distances less than 3°, equipped with three components seismometers, were selected and analyzed. The first step of the procedure is the preparation of the data includes the deconvolution of instrument response, the integration of the velocity to displacement and the rotation of the horizontal components to radial and transverse. Then the method uses the long period part of the signal to invert. The analysis was performed using the model suggested by Haslinger [25]. The quality of the results of moment tensor solutions can be evaluated by considering the average misfit and the compensated linear vector dipole (CLVD). For each solution, there is a quality code that consists between the letters A – D, for the minimum misfit and between the numbers 1 – 4 for the percent of CLVD [26], [27].

a. Kefallinia Seismic Sequence

The area of Kefallinia is characterized by too high seismicity, as shown by the past, e.g. the seismic action of August 1953 with earthquakes of magnitude 6.5, 6.8 and 7.2 leveled Kefalonia, Zande and Ithaca and caused about 480 human casualties. The geodynamics and seismotectonic of the area are particularly complex [3], [18]. After the destructive sequence of 1953, the strongest earthquakes that have taken place in the wider area are the one west of Cephalonia on 17.1.1983 with M_L=7.0, [13], [10], [28] and the one on 18.11.1997 with M_L=6.6 in the Strofades islands. The recent earthquake filled a seismic gap in the area.

On January 26, 2014 (13:55, UTC) two strong earthquakes of magnitude M_w=6.1 and M_w=5.2 (18:45, UTC) occurred in the island of Kefallinia, central Ionia Sea. These events induced extensive structural damages, mainly in the western and central parts. Eight days later on February 3, 2014 (03:08, UTC) a second strong event with a magnitude similar to the first (M_w=6.0) happened at the north section of Lixouri town. The geographical coordinates for the first events were manually relocated for this study and found φ=38.252°N, λ=20.443°E at depth 16 km. These two earthquakes (M_w=6.1 and M_w=6.0) occurred in the Kefallinia island of as the destructive events of 1953. In the first dayw og August 1953 (9th and 12th August), three earthquakes of magnitude 6.4, 6.8 and 7.2 [2] took place in Cephalonia,. For these three strong events, the source parameters were calculated and compared to the observed solutions from other institutes, and for the majority of them, a good agreement was found (Table 2). A large number of aftershocks followed these events. We note that for the first month, 2462 events were recorded and analyzed, while from the beginning of the sequence until the end of 2019 have taken place more than 17.000 events, recorded and viewed as a point cloud [29], [30] in Figure 2.

Preprints (www.preprints.org) | NOT PEER-REVIEWED | Posted: 4 September 2020 doi:10.20944/preprints202009.0080.v1

According to the first results, the peak ground acceleration may have exceeded 0.54g from the records of the LXRA accelerometers, while after the second event (03/02/2014) the peak ground acceleration was calculated at 0.68g from the recordings of the same station, [31].

The seismic sequence of Kefallinia in 2014 is evolving into a seismic area with a general direction from NW to NN and which is the continuation to the NN of the seismogenic area of Lefkas in 2003.

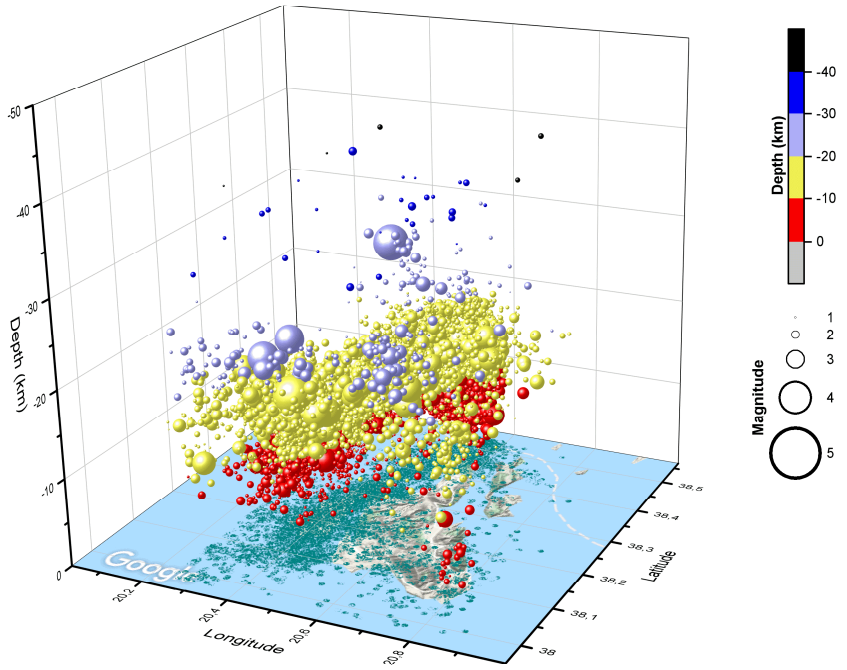

Figure 2: Distribution of epicenters for the seismic sequences in Kefallinia Island for the time period 26/01/2014 – 31/12/2019 with the total number of events N = 19.000. With red color marks the epicenter with depth under 10 km, with yellow color the epicenter of this sequence with depths between 10km < d< 20km and with blue color the epicenters with depths between 30km < d< 40km. All the depths of the epicenters were taken as they calculated from the manual analysis of the National Observatory of Athens, https://bbnet.gein.noa.gr/HL/databases/database by selecting the study area and the time interval.

From this catalogue and for the largest events (M_w > 3.8) the activation fault, the Source Parameters, the Seismic Moment (M_0) and the Moment Magnitude (M_w) were calculated, using the Moment tensor inversion [26].

Table 2: Comparison of this study results to a List of Moment tensor solutions published by various institutes for the three strong earthquakes in time period January – February 2014, in Kefallinia island Ionian Sea. Source: EMSC – CSEM, http://www.emsc-csem.org/Earthquake/tensors.php?id=357329&id2=kr068;INFO .

Kefallinia Earthquake (26/01/2014, 13:55:43.04, UTC) M_w = 6.1

Institute	Lat (°)	Lon (°)	M_w	M_0 (dyn*cm)	Depth (km)	Strike (°)	Dip (°)	Rake (°)	Strike (°)	Dip (°)	Rake (°)

Preprints (www.preprints.org) | NOT PEER-REVIEWED | Posted: 4 September 2020 doi:10.20944/preprints202009.0080.v1

This Study	**38.2520**	**20.4430**	**6.1**	**1.51E+25**	**13**	**23**	**68**	**175**	**115**	**85**	**22**
NOA	38.2200	20.3900	6.0	1,25E+28	6	18	67	164	114	75	24
HARV	38.1500	20.3600	6.1	2.04E+25	14	20	65	177	111	87	25
INGV	38.1700	20.3700	6.1	1.70E+25	10	290	81	-1	20	89	-171
KOERI	38.2830	20.5980	5.8	9.57E+24	16	16	87	-174	286	84	-3
GFZ	38.2500	20.4500	6.1	2.00E+25	17	289	85	4	198	86	175
CPP	38.2000	20.4000	6.2	2.12E+25	19	10	49	159	114	74	42
GEOAZUR	38.2080	20.4250	6.2	2.12E+25	6	15	68	165	111	76	22
AUTH	38.2600	20.5900	6.1	1,36E+28	10	286	90	-5	16	85	-180
UOA	38.2133	20.4672	6.1	2.03E+25	16	30	70	169	124	80	20

Kefallinia Earthquake (26/01/2014, 18:45:08.02, UTC) M_w = 5.3

Institute	Lat (°)	Lon (°)	M_w	M_0 (dyn*cm)	Depth (km)	Strike (°)	Dip (°)	Rake (°)	Strike (°)	Dip (°)	Rake (°)
This Study	**38.1423**	**20.2812**	**5.2**	**5,99E+23**	**20**	**19**	**62**	**170**	**114**	**81**	**28**
NOA	38.2360	20.4417	5.3	1,03E+27	6	149	64	65	16	35	131
HARV	38.1000	20.2500	5.5	2.02E+24	17	16	39	138	141	65	59
INGV	38.1200	20.2800	5.5	2.20E+24	17	15	38	139	140	66	60
GFZ	38.2900	20.3400	5.4	1.40E+24	15	173	50	91	352	40	89
AUTH	38.2300	20.3700	5.3	1.41E+24	9	20	39	123	160	58	66

Kefallinia Earthquake (03/02/2014, 03:08:44.66, UTC) M_w = 6.0

Institute	Lat (°)	Lon (°)	M_w	M_0 (dyn*cm)	Depth (km)	Strike (°)	Dip (°)	Rake (°)	Strike (°)	Dip (°)	Rake (°)
This Study	**38.2527**	**20.3948**	**6**	**2.46E+24**	**20**	**20**	**67**	**174**	**112**	**84**	**23**
NOA	38.2527	20.3948	5.9	1,02E+28	3	13	75	163	108	73	15
HARV	38.1200	20.3700	6.0	1.49E+25	12	12	45	154	120	72	48
INGV	38.2000	20.3900	6.1	2.00E+25	8	13	43	161	118	77	49
KOERI	38.2600	20.3200	5.8	9.57E+24	60	317	66	59	193	38	139
GFZ	38.2300	20.3900	6.0	1.30E+25	14	183	56	138	300	56	43
CPP	38.3000	20.3000	6.4	4,27E+25	15	142	82	84	355	10	122
AUTH	38.2700	20.3200	6.0	9.64E+24	7	287	87	-3	17	87	-177
UOA	38.2689	20.3881	5.9	9.60E+24	5	35	62	175	127	86	28

Immediately after the earthquake on January 26, 2014, in the area of Paliki of Kefallinia, the Geodynamic institute sent a team of scientists and technicians and installed a portable network (Figure 3) of four stations (KEF1, KEF2, KEF3 and KEF4), since the number of existing permanent stations was insufficient for detailed recording of aftershock – seismic activity. The significant result of the installation of the portable network was the possibility of recording thousands of earthquakes (N > 8.000) over a year, with magnitudes M > 1.0. The geographical distribution of the seismological portable network and the stations of the permanent seismological network whose data were used for the inversion appear in Figure 3.

Using the methodology, described in the previous section 2.2.1 and in the study [22], the Source Parameters (φ, δ, λ), the Moment Magnitude (M_w), the Seismic Moment (M_0) and the Depth were calculated and presented in Figures 4,5,6 regarding the three strongest earthquakes in Kefallinia Island.

Preprints (www.preprints.org) | NOT PEER-REVIEWED | Posted: 4 September 2020 doi:10.20944/preprints202009.0080.v1

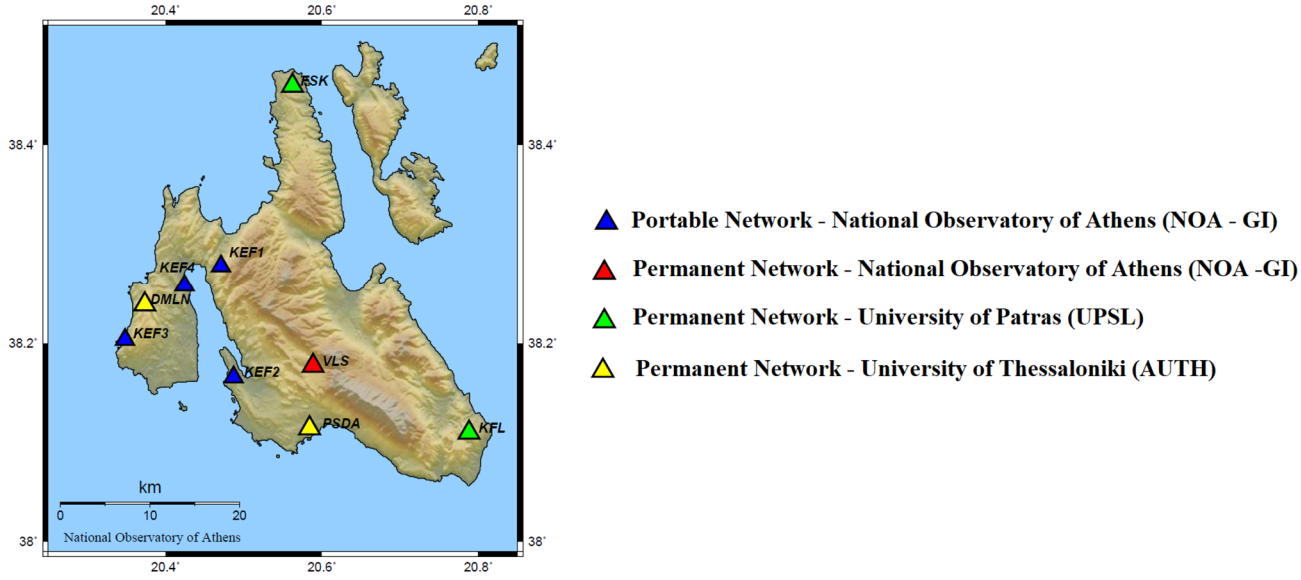

Figure 3: Map of permanent and portable network of Seismological Stations in Ionian Island, Greece.

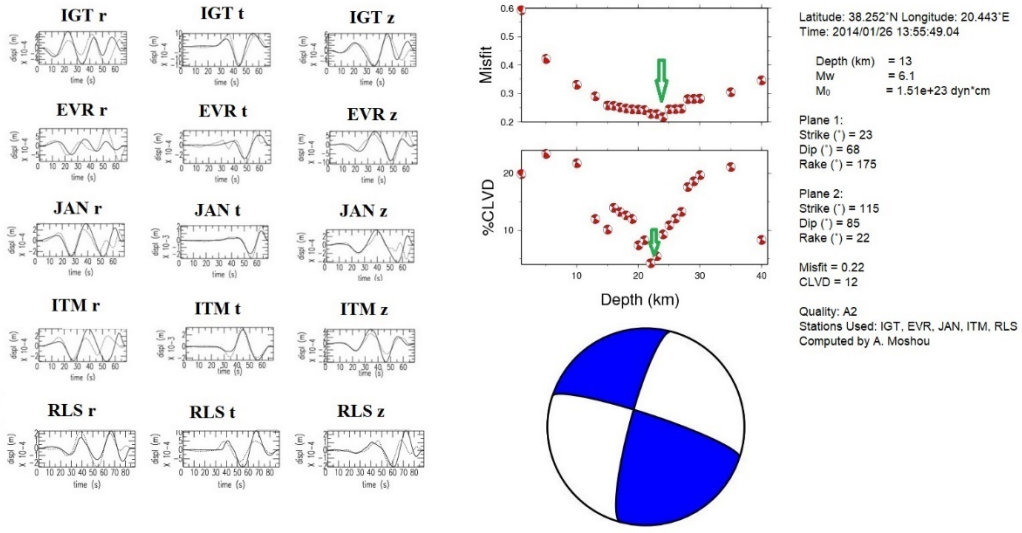

Figure 4: Moment tensor solution of the 26 January 2014 (13:55 UTC) earthquake. The selected solution is highlighted with the green arrow in the misfit/CLVD-versus-depth diagrams (center-up). The summary of the solution and the corresponding beach ball are shown in center-low. At left, the observed and synthetic displacement waveforms (continuous and dotted lines respectively) are shown, at the inverted stations for the radial, tangential and vertical components. At Left-Center-Right & Up-Middle-Low the summary of the solution and the fault plane solution as lower hemisphere equal – area projection, are depicted.

On 26 January 2014 (18:45 UTC), a few hours later from the first event a second of magnitude M_w = 5.2 occurred in the same region. Using waveforms from HUSN, the epicenter was manually located at 38.1423°N, 20.2812°E. Broadband recordings from the HUSN network were collected and those at epicentral distances less than 3° degrees were selected. For the inversion method, 5 stations were used with good azimuthal coverage. Reverse type faulting was revealed after applying the previous methodology. The obtained focal mechanism is φ=19°, δ=62° and λ=170°. The seismic moment is equal to $M_o = 5.99 \cdot 10^{23}$ dyn·cm, for a focal depth equal to 20 km. The inversion resulted a DC equal to 89%, while the compensated linear vector dipole was equal to 9% (Figure 5).

Preprints (www.preprints.org) | NOT PEER-REVIEWED | Posted: 4 September 2020 doi:10.20944/preprints202009.0080.v1

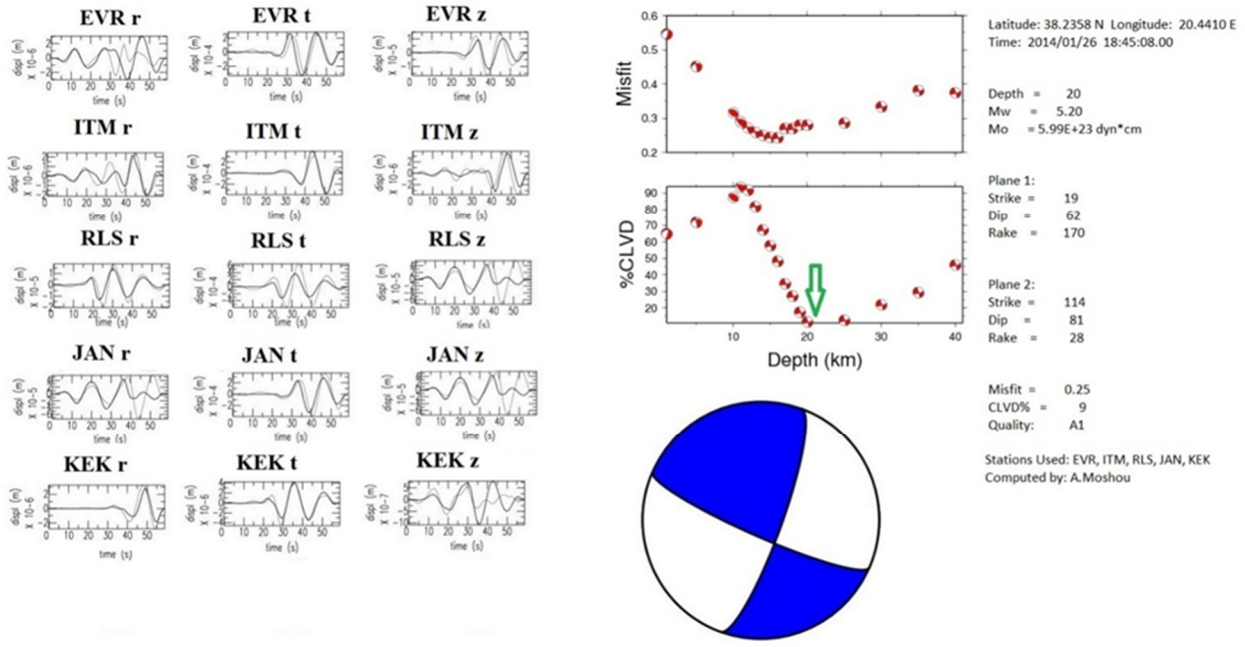

Figure 5: Moment tensor solution of the 26 January 2014 (18:45 UTC) earthquake. The selected solution is highlighted with the green arrow in the misfit/CLVD-versus-depth diagrams (center-up). The summary of the solution and the corresponding beach ball are shown in center-low. At left, the observed and synthetic displacement waveforms (continuous and dotted lines respectively) are shown, at the inverted stations for the radial, tangential and vertical components. At Left-Center-Right & Up-Middle-Low the summary of the solution and the fault plane solution as lower hemisphere equal – area projection, are depicted

Next, we present the results of inversion for the third-largest earthquake of this seismic sequence. This earthquake showed specificity as to the application of the method mainly because of its geographical position. The epicenter was calculated in the N – W part of the Kefallinia Island, according to the National Observatory of Athens (φ = 38.2462° N, λ = 20.3958° E). Due to bad azimuthal coverage of the Greek stations, trials were made for some fault plane solutions being recalculated by adding records either of Italian stations, either in mixed epicentral distances, more than 300 km, thus extending our azimuthal coverage to the west and south of the epicenter. To compute the focal mechanism 6 stations of three components, each one was used in epicentral distances between 130 and 380 km to determine the source parameters of this event. The source parameters were calculated using the method of moment tensor inversion outlined previously. The best fit solution is: strike=176°, strike=58°, rake=145° and the focal depth is calculated at 12 km. The seismic moment is determined M_o=1.63·10^{25} dyn·cm and the calculated double couple (DC) was found equal to 88%, while the compensated linear vector dipole (CLVD) to 12%. The results of the applied procedure are presented in Figure 6.

Preprints (www.preprints.org) | NOT PEER-REVIEWED | Posted: 4 September 2020 doi:10.20944/preprints202009.0080.v1

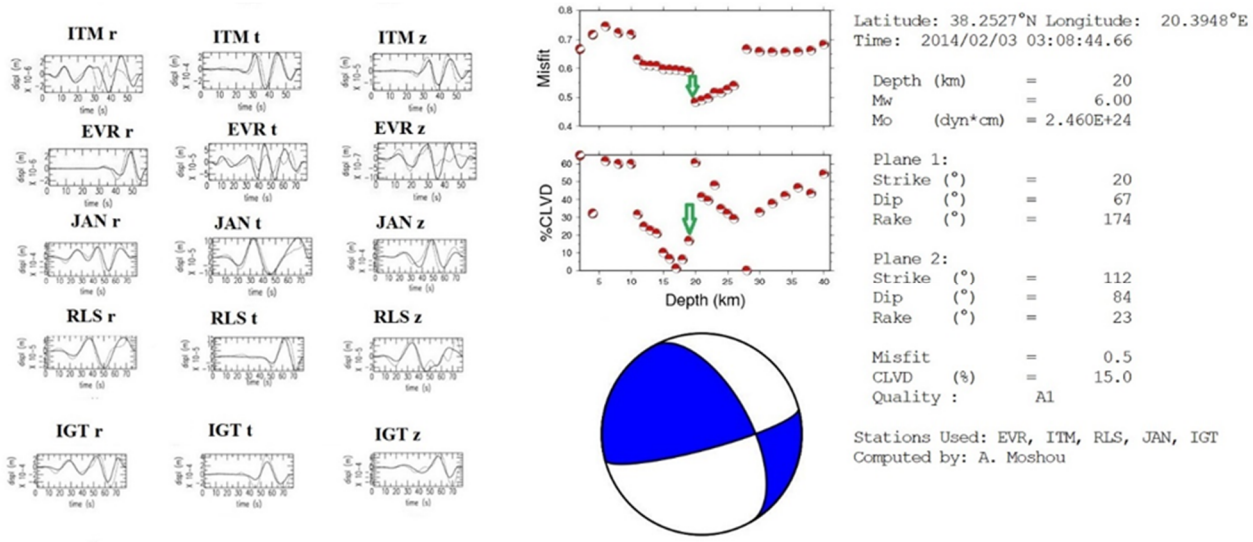

Figure 6: Moment tensor solution of the 03 February 2014 (03:08 UTC) earthquake. The selected solution is highlighted with the green arrow in the misfit/CLVD – versus – depth diagrams. Down of this are appeared the summary of the solution and the corresponding beach ball. To the left of misfit/CLVD diagrams observed and synthetic displacement waveforms (continuous and dotted lines respectively) are shown, at the inverted stations for the radial, tangential and vertical components. At the lower part of the figure the summary of the solution and the fault plane solution as lower hemisphere equal – area projection, are depicted

Figures 7 and 8 represent the spatiotemporal evolution of the seismicity (2014 – 2019) as a function of Latitude and depth, respectively.

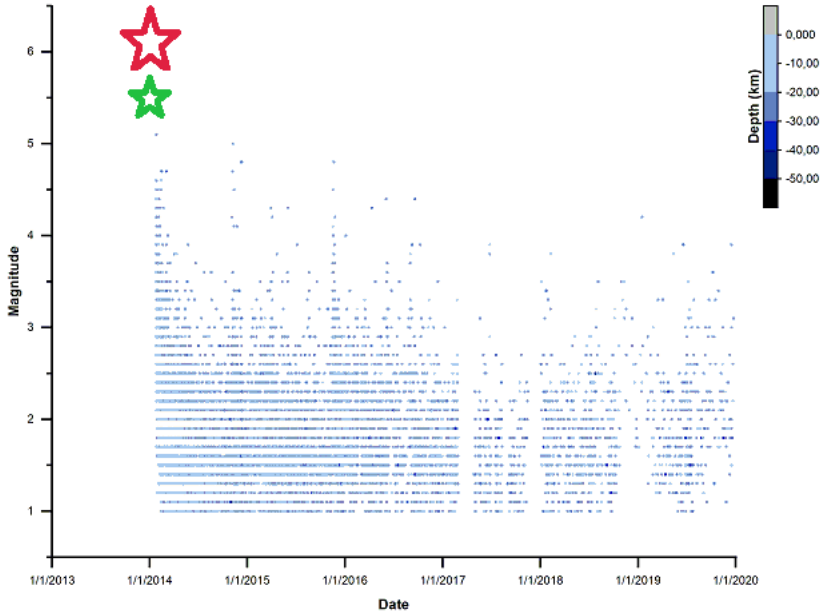

Figure 7: Spatio – Temporal evolution of the seismicity as a function of magnitude. The red star corresponds to the main event of 26 January 20014 and the green star denotes the 03 February 2014.

Preprints (www.preprints.org) | NOT PEER-REVIEWED | Posted: 4 September 2020 doi:10.20944/preprints202009.0080.v1

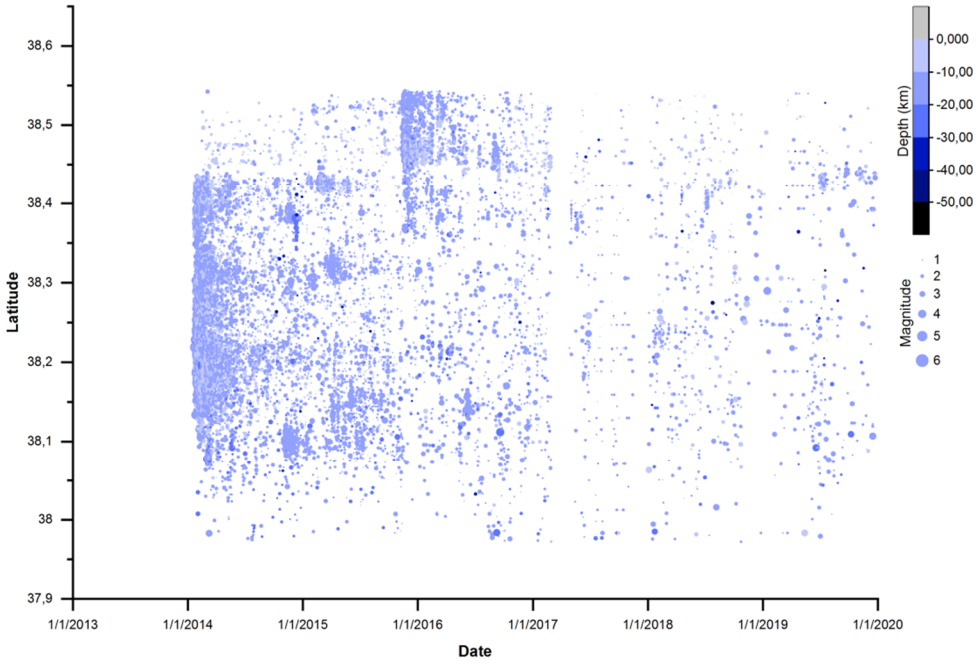

Figure 8: Spatio – Temporal evolution of seismicity as a function of latitude.

b. Lefkas Island

A strong earthquake with magnitude M_w=6.4 occurred in Lefkas Island, Greece. The geographical coordinates, as they calculated from the manual analysis of the Institute of Geodynamics – NOA (http://bbnet.gein.noa.gr/alerts_manual/2015/11/evman151117071007_info.html) are φ=38.6655°N, λ =20.6002°E at a depth 10km. A few hours later, a second strong event with magnitude M_L=5.0 occurred in the same region. These earthquakes caused a lot of structural damage to the villages of Agios Petros, Athani, Dragano and Komilio [30]. Environmental effects include liquefaction, extensive rock falls and landslides. No surface ruptures were found in the field. The most recent strong earthquake occurred on August 14, 2003 with a magnitude of M_w=6.2, offshore the western coast of Lefkas Island, causing severe damages around the whole island [31], [32], [33], [34], [35], [36], [37].

These events were followed by a rich seismic sequence for the following days. More specifically, from 17/11/2015 until the end of the month 837 events were recorded, while for the first 24 hours, the recorded events were 206. The 3D distribution of the epicenters compared to depths and the magnitudes is shown in Figure 9.

All the focal mechanisms from events with magnitude M_w>4.0 were calculated using the proposed methodology (Appendix A, Table A2). The source parameter and the focal mechanism for the main event is shown in Figure 10. For this purpose, the data of 6 stations of three components each one in epicentral distances less than 350 km were used. The source parameters were calculated using the method of moment tensor inversion outlined previously. For the main event, the inversion indicates the activation of a strike slip type faulting. The best fit solution is strike=290°, strike=88°, rake=-12° and the focal depth is calculated at 10 km. The seismic moment is determined Mo = $4.402 \cdot 10^{28}$ dyn·cm and the calculated double couple (DC) was found equal to 93%, while the compensated linear vector dipole (CLVD) to 7%. The result of the applied modeling is presented in Figure 9.

Preprints (www.preprints.org) | NOT PEER-REVIEWED | Posted: 4 September 2020 doi:10.20944/preprints202009.0080.v1

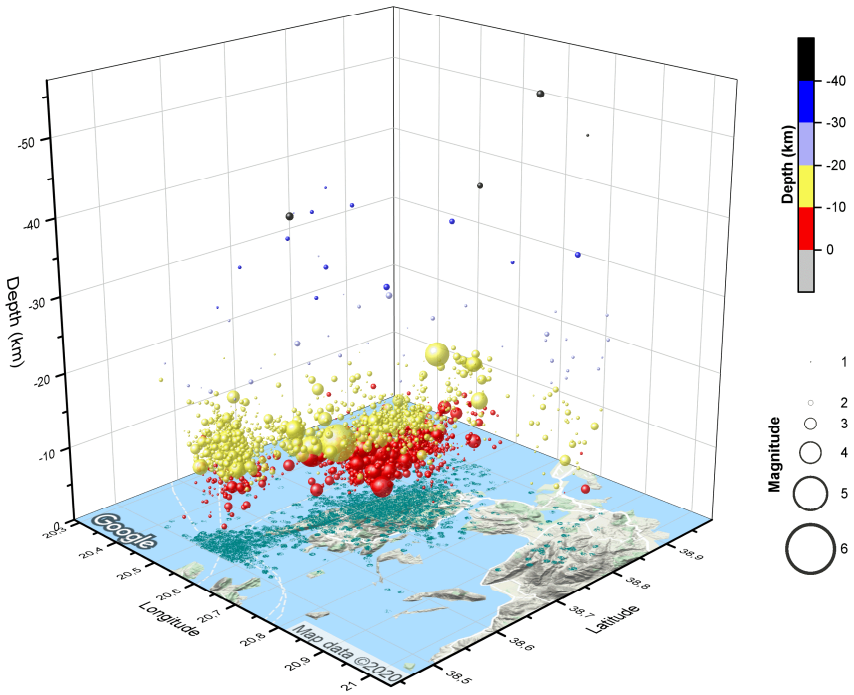

Figure 9: Distribution of epicenters for the seismic sequences in Lefkas Island for the time period 17/11/2015 – 31/12/219 with total number of events N = 1427. With red color marks the epicenter with depth under 10 km, with yellow color the epicenter of this sequence with depths between 10km < d< 20km and with blue color the epicenters with depths between 30km < d< 40km. All the depths of the epicenters were taken as they calculated from the manually analysis of the National Observatory of Athens, https://bbnet.gein.noa.gr/HL/databases/database ,by selecting the study area and the time interval

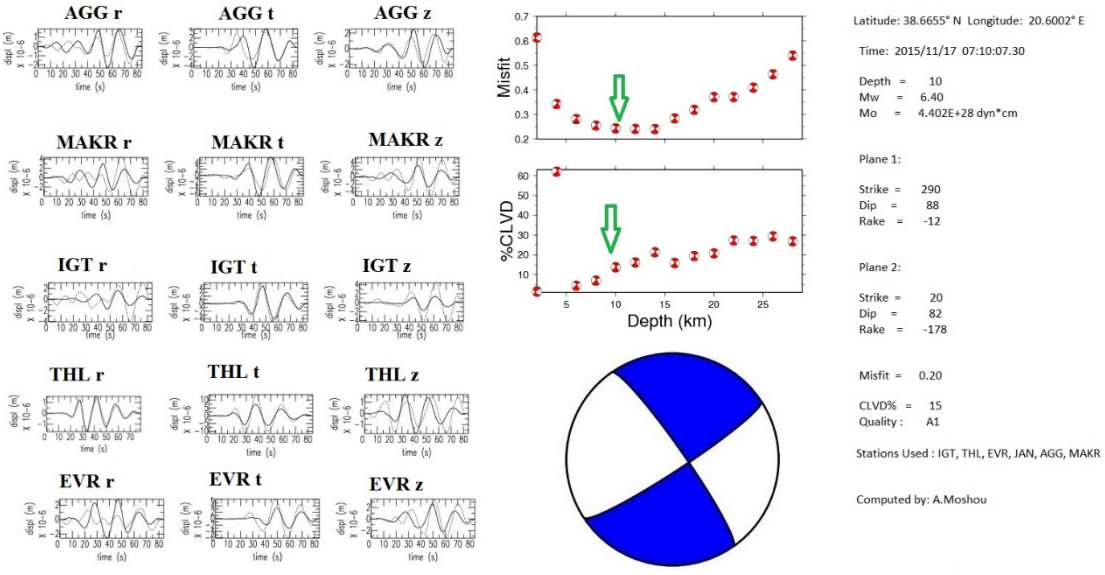

Figure 10: Moment tensor solution of the 17 November 2015 (07:10 UTC) earthquake. The selected solution is highlighted with the green arrow in the misfit/CLVD-versus-depth diagrams (center-up).

Preprints (www.preprints.org) | NOT PEER-REVIEWED | Posted: 4 September 2020 doi:10.20944/preprints202009.0080.v1

the summary of the solution and the corresponding beach ball are shown in center-low. At left, the observed and synthetic displacement waveforms (continuous and dotted lines respectively) are shown, at the inverted stations for the radial, tangential and vertical components. At Left-Center-Right & Up-Middle-Low the summary of the solution and the fault plane solution as lower hemisphere equal – area projection, are depicted.

c. Zande Seismic Sequence

On 25 October 2018 (22:54 UTC) a strong shallow earthquake with magnitude Mw=6.7 occurred offshore Zande (Ionian Sea, Greece). The epicenter calculated was located φ=37.341°N, λ=20.512°E, 40km southwest of the island of Zande, Ionian Sea, Greece, [38], [39], [40], [41].

A large number of aftershocks followed this event in Figure 11. The most recent seismic sequence was occurred during April – May 2006. It consists of four moderate earthquakes ($5.3 \leq M_w \leq 5.7$) that were followed by significant seismic activity. Those focal mechanism were calculated in the study [42].

All the focal mechanisms from events with magnitude $M_w > 4.5$ were calculated (Appendix A, Table A3). To determine the source parameters, the data of 5 stations of three components each one in epicentral distances less than 350 km were used. The source parameters were calculated using the method of moment tensor inversion outlined previously. Thrust type faulting was revealed after applying moment tensor inversion. The best fit solution is strike=123°, strike=42°, rake=30° and the focal depth is calculated at 17 km. The seismic moment is determined $M_0 = 1.45 \cdot 10^{26}$ dyn·cm and the calculated double couple (DC) was found equal to 92%, while the compensated linear vector dipole (CLVD) to 8%. The result of the applied modeling is presented in Figure 12.

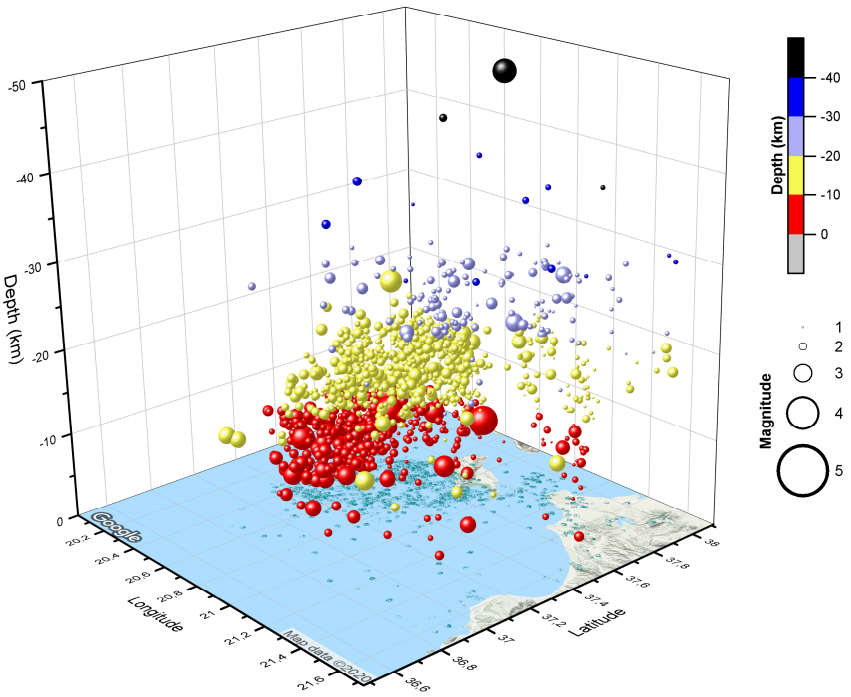

Preprints (www.preprints.org) | NOT PEER-REVIEWED | Posted: 4 September 2020 doi:10.20944/preprints202009.0080.v1

Figure 11: Distribution of epicenters for the seismic sequences in Zande Island for the time period 25/10/2018 – 31/12/2019 with total number of events N = 10.460. With red color marks the epicenter with depth under 10 km, with yellow color the epicenter of this sequence with depths between 10km < d< 20km and with blue color the epicenters with depths between 30km < d< 40km. All the depths of the epicenters were taken as they calculated from the manual analysis of the National Observatory of Athens dataset, https://bbnet.gein.noa.gr/HL/databases/database by selecting the study area and the time interval.

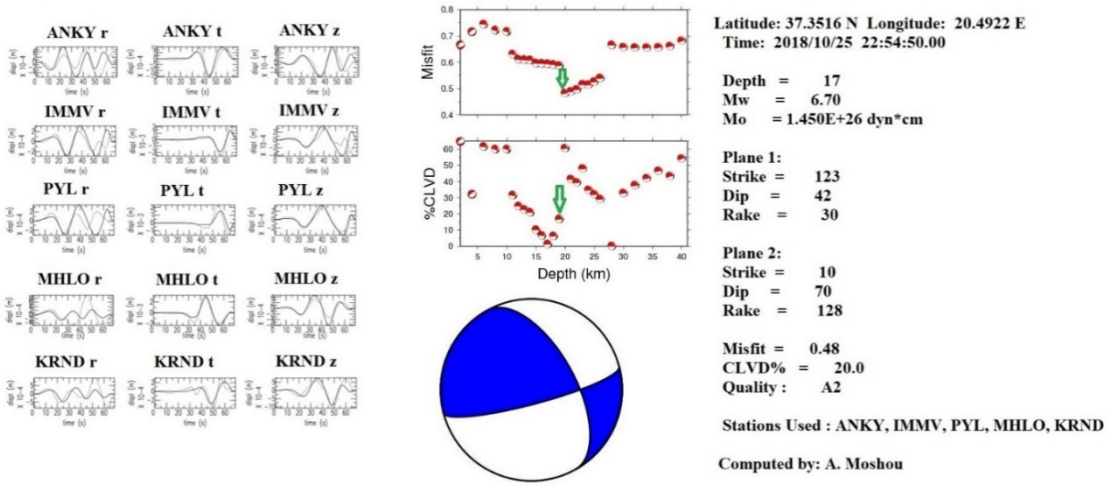

Figure 12: Moment tensor solution of the 25 October 2018 (22:54 UTC) earthquake. The selected solution is highlighted with the green arrow in the misfit/CLVD-versus-depth diagrams (center-up). the summary of the solution and the corresponding beach ball are shown in center-low. At left, the observed and synthetic displacement waveforms (continuous and dotted lines respectively) are shown, at the inverted stations for the radial, tangential and vertical components. At Left-Center-Right & Up-Middle-Low the summary of the solution and the fault plane solution as lower hemisphere equal – area projection, are depicted.

2.2 GPS Data and methods

The GPS data (30-s sampling interval) were collected and processed from stations VLSM (Valsamata Cephalonia), SPAN (Spanohori Lefkas), PONT (Ponti Lefkas) shown in Figure 13, which belong to the national geodetic network of the Institute of Geodynamics – National Observatory of Athens (NOANET; http://www.gein.noa.gr/services/GPS/noa_gps.html). The exact location and instruments information of the permanent stations are shown in Table 3.

Table 3: Characteristics of GNSS stations in Ionian. Station coordinates are in decimal degrees; height is in m.

Name	Location	LAT	LON	Height	Antenna	Receiver	Data Start	Data End
VLSM	Valsamata (Kefallinia	38.176	20.588	437.19	LEIAS 10, NONE	LEICA GR10	1/1/2014	30/12/2019
PONT	Ponti (Lefkas)	38.619	20.585	48.81	LEIAX1202, GG DONE	LEICA GRX 1200PRO	1/1/2014	30/12/2019
SPAN	Spanochori (Lefkas)	38.781	20.673	451.34	LEIAX1202, GG DONE	LEICA GRX 1200PRO	1/1/2014	30/12/2019

Preprints (www.preprints.org) | NOT PEER-REVIEWED | Posted: 4 September 2020 doi:10.20944/preprints202009.0080.v1

After the collection of GPS raw data from the online repository, a preprocessing procedure was applied to assure the best quality of post-processing results. TEQC software [43] was used to identify data incompatibilities, excess multipath and data gaps.

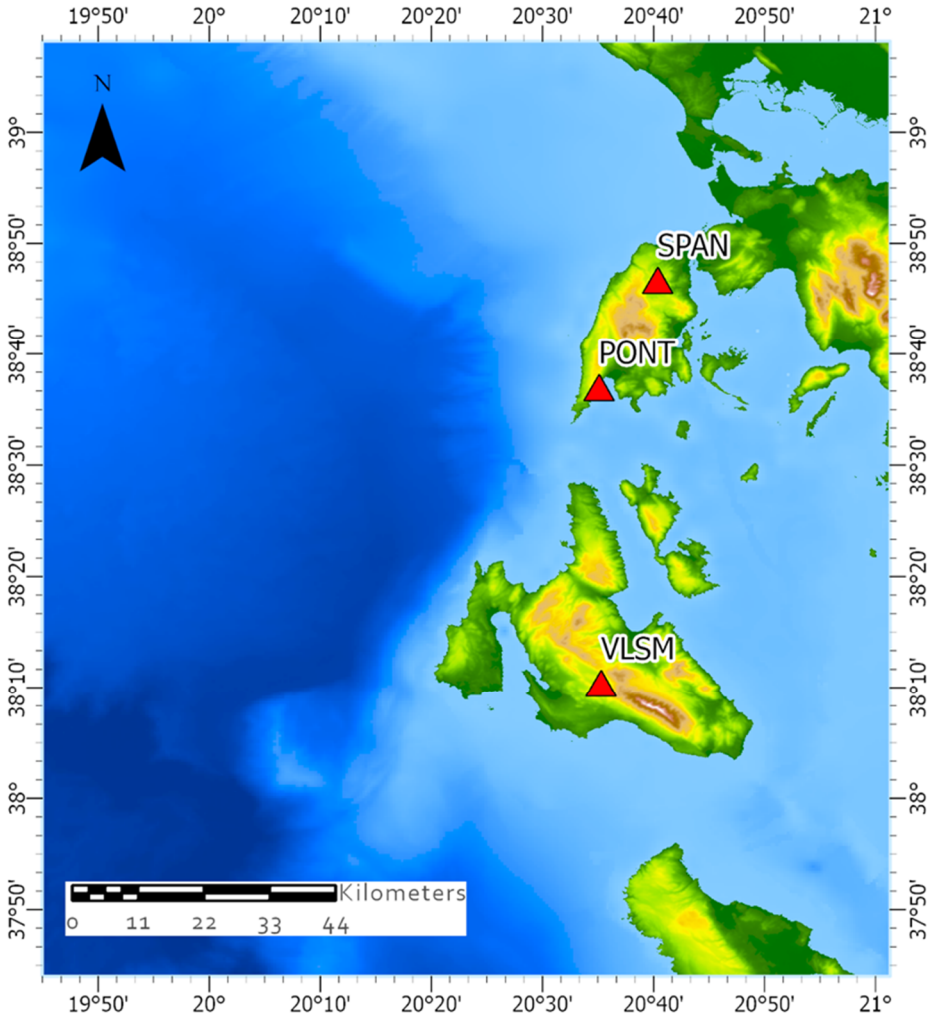

Figure 13. Map of Permanent GNSS Stations VLSM (Valsamata Cephalonia), PONT (Ponti Lefkas), SPAN (Spanohori Lefkas)

2.2.1 Processing of GPS data

GIPSY/OASIS II software (ver. 6.4) developed by Jet Propulsion Laboratory (JPL; http://gipsy-oasis.jpl.nasa.gov) [44] was used to process our data from GPS. The precise Point Positioning strategy (PPP) [45] is used by the post-processing software. The main advance of this method is that only a single specific station is needed to produce results, rather than analyzing tens of stations in a technique like DGPS, which also saves valuable computational resources and time.

The format of the GPS Data was RINEX 2.11 from all the three stations (VLSM, PONT, KLOK), a non – fiducial high precision clock and orbit files that were used (flinnR_nf from JPL). According to international guidelines and experience [46] (e.g., Hill and Blewitt, 2006; (a value of 5x10-8 cm/sec2 random walk noise is recommended) zenith, tropospheric estimation was used. A troposphere mapping function GPT2 (Global Pressure and Temperature Mapping Function) [47] Rozsa, 2014 was used, which was shown to be better than the NIELL mapping function [48] and provides similar results as the VMF1 model (Vienna Mapping Function). Because we analyze long-term recording GNSS stations [49] (we keep the advantage not to maintain a tropospheric database for this purpose), the use of GPT2 was found more appropriate. A lower elevation angle cutoff of 10o was

Preprints (www.preprints.org) | NOT PEER-REVIEWED | Posted: 4 September 2020 doi:10.20944/preprints202009.0080.v1

used to eliminate the near-field multipath effect. Also, a receiver antenna calibration file was calculated and generated for each station separately from the IGS atx file (from http://www.igs.org/wg). WahrK1 [50] tide model was used and (OcnldCpn) ocean load tide model was added which uses 11 tidal frequencies to infer other frequencies; After the post-processing procedure a reference frame transformation to ITRF2014 took place for each station and finally the time series was plotted in Figure 14.

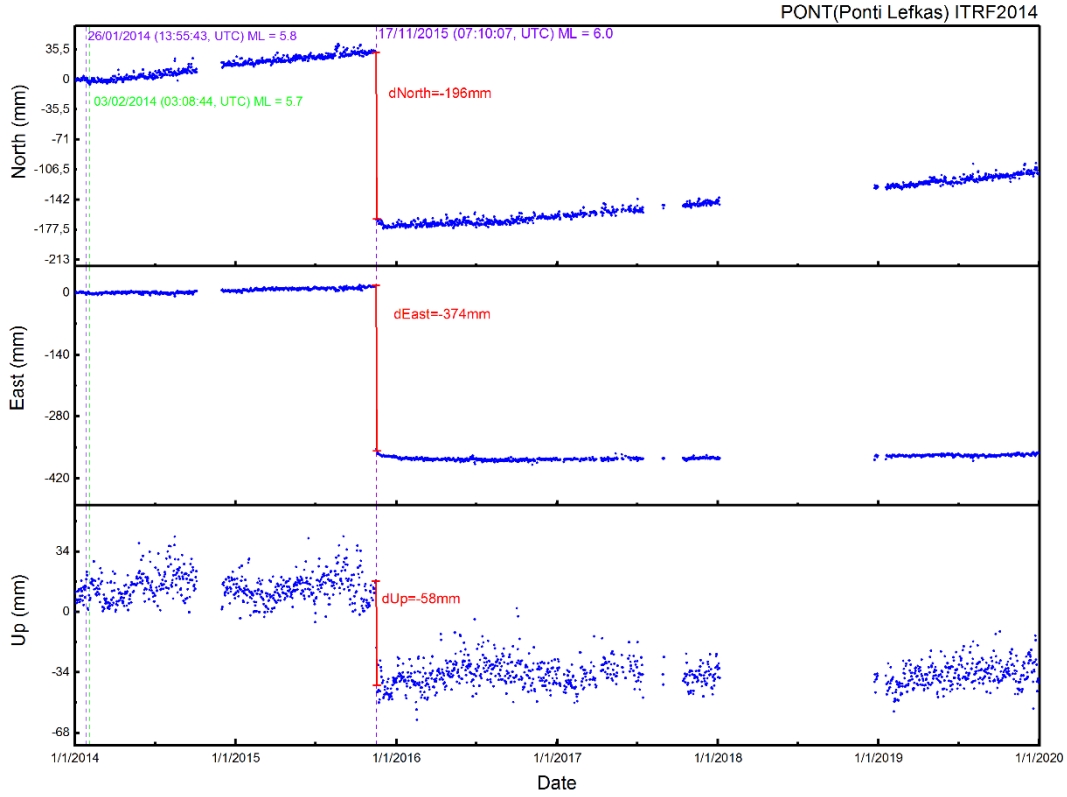

(a)

Preprints (www.preprints.org) | NOT PEER-REVIEWED | Posted: 4 September 2020 doi:10.20944/preprints202009.0080.v1

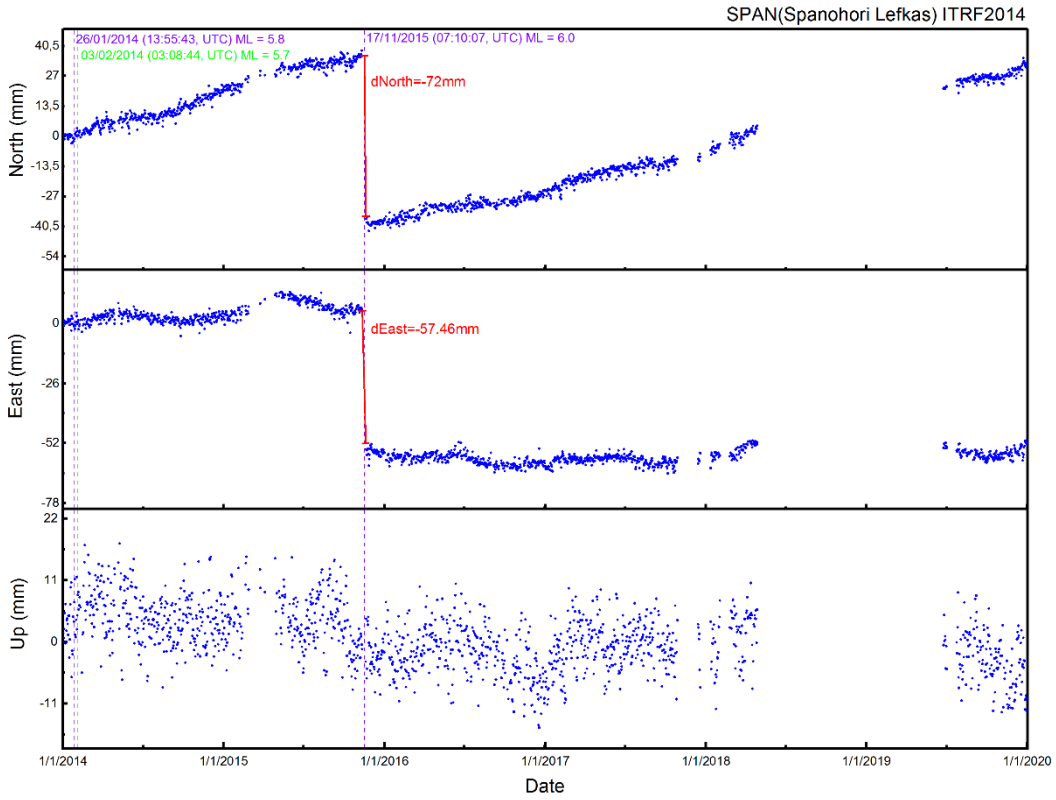

340 **(b)**

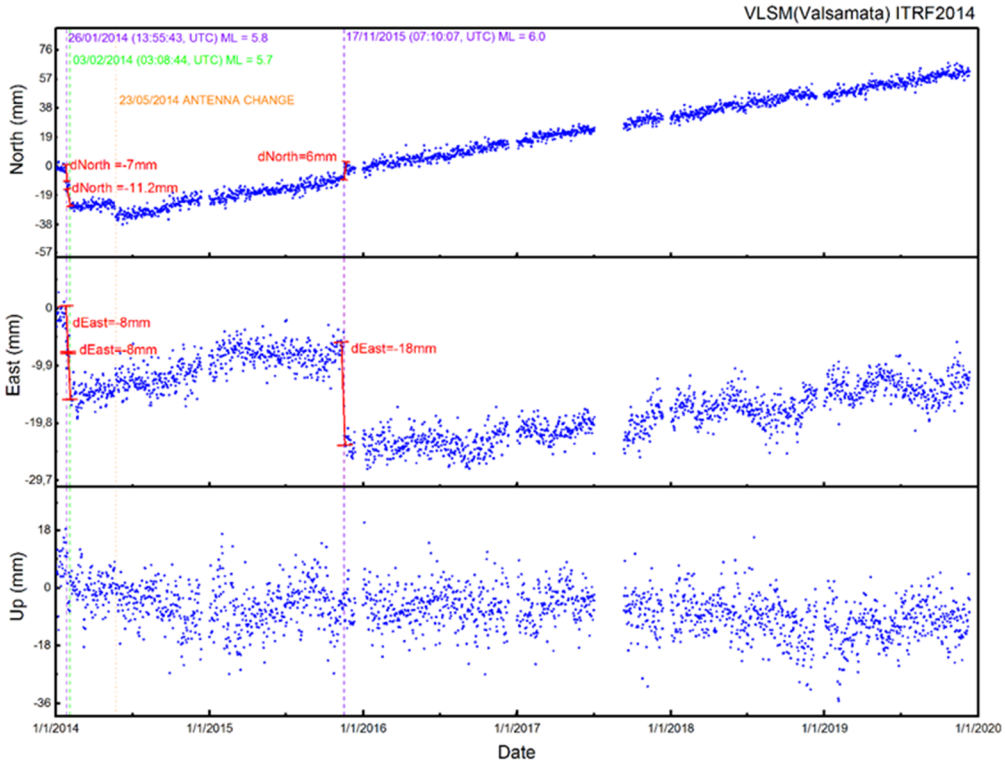

341
342 **(c)**

Preprints (www.preprints.org) | NOT PEER-REVIEWED | Posted: 4 September 2020 doi:10.20944/preprints202009.0080.v1

Figure 14. GNSS Time Series of permanent stations: (a) PONT, (b) SPAN (c) VLSM. Vertical lines show the significant earthquakes at 2014 and 2015 and also shows in 2014 the effect on time series of antenna change at station VLSM. The displacement occurred was marked with a vertical red line.

2.4 Clustering of the Seismic Data

Modern statistical analysis methods can be also applied to the collected datasets. SOM [51], [52], k-Means [53], or other clustering techniques from Machine Learning are used by researchers to retrieve deeper knowledge of the seismic behavior. Here, the clustering of the data is done by applying a self-organized map (SOM) artificial neural network (ANN) in order to define the major areas from where the events originate. Figure 15 shows the distribution of over 9000 events during 2019 in the island of Zande, indicating with circles the positions of the top 20 events with the highest magnitude (Fig. 15a).

In order to use the SOM tool, the Lat-Long data were first transformed to X-Y data and then normalized in the [0,1] range. The X-Y locations of these events were introduced in a number of different SOM networks. SOM training automatically adjusts the network weights and creates a map of the cluster centers. Figures 15b & 15c present the results of two SOM of size 2 & 3 with 4 & 9 nodes respectively.

From figure 15, we can see how a machine learning technique like SOM can locate larger or smaller neighborhoods (classes) of events and define their "center of gravity" in terms of population in the X-Y plane, and, how closely the M_L tool results can relate to the most significant events, in terms of magnitude.

The application of modern statistical tools can be further extended to more tools (k-Means or deep learning techniques), as well as, to more than 2 dimensions, e.g. the depth and/or the time of the event, in order to map the spatio-temporal clustering of the events and their epicenters and reveal further properties of these events and moreover, study the clustering centers displacement with respect to time and magnitude.

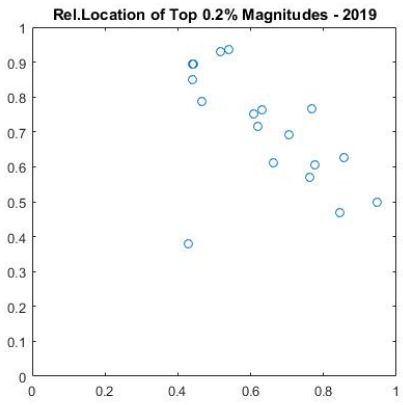

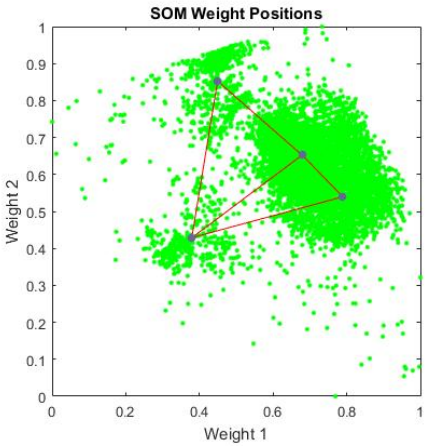

(a) **(b)**

Preprints (www.preprints.org) | NOT PEER-REVIEWED | Posted: 4 September 2020 doi:10.20944/preprints202009.0080.v1

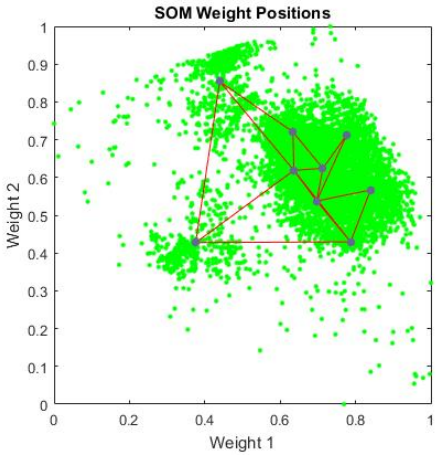

(c)

Figure 15: SOM results of 2019 events on the normalized X-Y (Weight1-Weight2) plane: **(a)** the 0.2% major events of highest magnitude, **(b)** SOM(2) with 4 nodes, and **(c)** SOM(3) with 9 nodes.

3. Conclusions

The focal mechanisms of small earthquakes, west of Lefkas to the north Kefallinia, are mainly characterized by horizontal slip faults [49], [50], [51]. Specifically, as demonstrated by the method, the right-hand horizontal shift fault west of Kefallinia receives an address ~ 40° North while for the department west of Lefkas, it turned out that the fault has a direction 20° North. This observation agrees with the study of [50] as well as the work of [45], [47]. Also, from the study of focal mechanisms [52], [53] indicates that west of Lefkas, the activation of a strike-slip fault occurred. East of Zande up to the western part of the Peloponnese predominate horizontal sliding mechanisms while in the bay of Zande, they respond mainly reverse burglary mechanisms [54]. Most of the earthquakes in the area are associated with one right-hand horizontal slip [55]. In the eastern part of the Ionian, there are surface earthquakes with activation, mainly horizontal slip faults. Finally, in the southern part inverted types of generating mechanisms are activated. The depth of the earthquakes studied in this area is between 12 and 30 km, which shows that they are increased compared to the usual depths are identified for surface earthquakes throughout Greece. In this study, the results of the analysis of the three aftershocks sequences are presented.

- The first of this is in the Western Kefallinia Island, Ionian Sea, at the SSW-wards continuation of the Lefkas segment of the Cephalonia Transform Fault Zone (CTFZ). More than 8.000 earthquakes occurred in the first year. The obtained results provided insights on the rupture mechanism, the temporal and spatial distribution of the seismic sequence. Source parameters that is focal depth, fault plane solution and seismic moment were determined by applying the moment tensor inversion methodology using regional data in distances less than 3°. The determined fault plane solutions represent the activation of a strike slip fault, and a depth distribution of the entire sequence ranges mainly between 10 – 20 km. These results are in good agreement with other studies in this region [54], [55], [56], [57]. For the same region and events, the GNSS data were used and analyzed. The results indicate an N – S displacement ~7mm and E – W displacement ~8mm take place at station VLSM also at earthquake 03/02/2014 (03:08:44, UTC) M_L = 5.7 a N – S displacement ~11.2mm and E – W displacement ~8mm take place at the same station and none of the other two stations significantly affected. It is obvious that the seismic sequence of Kefalonia in 2014 is evolving into a seismic area with a general direction from NW to NN.

- The second seismic sequence that analyzed is the Lefkas Island earthquake (17/11/2015, 07:10:07, UTC) to the southwestern part of Lefkas island. The analysis of the GNSS data showed a N

– S displacement ~196mm, a E-W displacement ~374mm and a Vertical displacement ~58mm take place at station PONT also a N – S displacement ~72mm and E – W displacement ~57.46 mm take place at station SPAN accordingly a S – N displacement ~6mm and E – W displacement ~18mm take place at station VLSM. These results are confirmed by the focal mechanism that has already been calculated as well as with the results of other studies [44].

- Finally, the earthquake sequence at the southern coast of Zande Island that lasted from October 2018 April until the end of 2019 was investigated. The focal mechanism solutions of the 18 strongest events ($M_w > 4.0$) for the period 2018 – 2019, located at depths ranging from 12 – 18km, support this hypothesis. The focal mechanism of the main event as well as for the strongest earthquakes, indicate the activation of a thrust type faulting with a component of strike slip. This study indicates that the October 25, 2018 $M_w = 6.7$ event ruptured the Hellenic megathrust. This event highlights the high degree of seismic coupling in the western region of the Hellenic Arc.

- The GNSS data also point to a similar pattern between the coseismic strain released during the 2014 until the end of 2019 event and the long-term (interseismic) strain accumulation along the west Hellenic Arc. Also, the fault-plane geometry is well constrained by GNSS. This is consistent with the distribution of the aftershocks.

- By applying Machine Learning techniques on our data, we can cluster the events and their epicenters, study further their properties and their variability over time, and also propose new or better positions to improve our portable stations network acquisition.

Funding:

This research received no external funding

Acknowledgments:

We acknowledge the use of Hellenic Unified Seismograph Network (HUSN) data and we would like to thank the NOA scientific personnel for phase picking.

We gratefully thank the operators of the European permanent seismic networks who make their data available through EIDA, http://www.orfeus-eu.org/eida . In this study data from the following Institutes were used.

- HL (NOA, Hellenic Seismic Network), doi:10.7914/SN/HL
- HT (Aristotle University of Thessaloniki Seismological Network), doi:10.7914/SN/HT
- HP (University of Patras, Seismological Laboratory), doi:10.7914/SN/HP
- HA (National and Kapodistrian University of Athens, Seismological Laboratory), doi:10.7914/SN/HA

Figures containing maps were drawn using the Generic Mapping Tools (GMT) software (Wessel and Smith, 1998).

We acknowledge concession for the use of ESRI products licensed to the Hellenic National Tsunami Warning Center, National Observatory of Athens, through the project "HELPOS - Hellenic Plate Observing System" (MIS 5002697). HELPOS is implemented under the Action "Reinforcement of the Research and Innovation Infrastructure", funded by the Operational Programme "Competitiveness, Entrepreneurship and Innovation" (NSRF 2014-2020) and co-financed by Greece and the European Union (European Regional Development Fund).

We thank the NOANET network for GNSS data.

Conflicts of Interest

The authors declare no conflict of interest

Appendix A

Table A1. Source Parameters of the main events as well as for the intermediate magnitudes for Kefallinia Seismic Sequence for the period 2014 – 2019. Nr is the event number. Lat and Lon are the geographical coordinates of each event, as they calculated by National Observatory of Athens; M0 is the seismic moment in dyn*cm, Mw is the moment magnitude; Strike, Dip, Rake of the two nodal planes is the seismic parameters as they calculated from the inversion; CLVD is the percentage of Compensated Linear Vector Dipole which describes seismic sources with no volume changes; Nr of stations is the number of stations used in inversion and finally the quality of the solution depending from the Misfit and the percentage CLVD

Nr	Origin		Location		Mo	M_w	Depth (km)		Plane 1			Plane 2			CLVD (%)	Nr of stations	Quality
	Date	Time	Lat (°)	Lon (°)	(dyn·cm)		Catalog	MT	Strike (°)	Dip (°)	Rake (°)	Strike (°)	Dip (°)	Rake (°)			
1	1/26/2014	13:55:42	38.2190	20.5320	1.51E+25	6.1	21.1	13	23	68	175	115	85	22	3	5	A1
2	1/26/2014	14:08:39	38.1880	20.5325	2.96E+22	4.3	18.9	12	20	64	170	114	81	26	15	4	B1
3	1/26/2014	14:21:58	38.2088	20.3787	9.52E+21	4.0	9.9	8	22	67	168	117	79	23	12	4	C1
4	1/26/2014	14:24:04	38.2532	20.3903	2.22E+22	4.2	14.5	14	19	62	170	114	81	28	16	4	B1
5	1/26/2014	14:41:39	38.2167	20.4757	2.22E+22	4.2	17.1	13	20	60	172	114	83	30	13	4	B1
6	1/26/2014	14:55:50	38.2132	20.4100	9.52E+21	4.0	14.2	14	23	68	176	115	86	22	12	4	B1
7	1/26/2014	14:59:25	38.3030	20.4753	7.35E+22	4.5	12.9	12	25	65	179	115	89	25	10	4	B1
8	1/26/2014	15:36:39	38.2363	20.4373	1.38E+22	4.1	17.1	13	18	64	170	112	81	26	8	5	C1
9	1/26/2014	18:45:08	38.2358	20.4410	5.99E+23	5.2	16.5	20	19	62	170	114	81	28	9	5	A1
10	1/26/2014	19:03:07	38.1873	20.4177	2.96E+22	4.3	17.1	13	20	69	169	114	80	21	12	5	A2
11	1/26/2014	19:12:04	38.2408	20.4002	4.06E+22	4.4	18.0	12	22	70	168	116	79	20	15	4	A1
12	1/26/2014	21:15:34	38.1337	20.3002	8.17E+22	4.6	10.4	11	23	65	170	117	81	25	14	4	B1
13	1/26/2014	21:42:12	38.1890	20.4862	9.52E+21	4.0	13.0	13	17	64	165	114	77	27	13	4	B1
14	1/26/2014	23:06:55	38.2398	20.4297	2.22E+22	4.2	18.3	13	24	65	174	117	85	25	12	4	A2
15	1/27/2014	9:47:38	38.1517	20.4025	1.38E+22	4.1	14.8	14	26	68	175	118	85	22	10	4	A1
16	1/27/2014	13:05:50	38.2308	20.4403	2.96E+22	4.3	11.1	11	19	69	169	113	80	21	8	4	B1
17	1/27/2014	15:39:34	38.3748	20.4222	2.22E+22	4.2	13.8	13	20	80	173	289	83	10	7	4	C1
18	1/28/2014	1:05:55	38.2542	20.4347	9.52E+21	4.0	15.1	12	20	65	172	113	83	25	12	4	B1
19	1/28/2014	5:12:53	38.2083	20.3817	2.96E+22	4.3	12.8	8	22	62	170	117	81	28	8	4	C1
20	1/28/2014	8:07:11	38.2138	20.5502	9.52E+21	4.0	15.3	11	23	60	172	117	83	30	13	4	A1
21	1/28/2014	14:49:33	38.2120	20.4552	9.52E+21	4.0	17.7	11	25	68	174	117	84	22	10	4	B1
22	1/28/2014	19:12:11	38.4048	20.5022	1.38E+22	4.1	10.6	12	17	64	176	109	86	26	12	4	A2
23	1/28/2014	22:22:37	38.4037	20.4885	2.22E+22	4.2	15.6	13	20	65	173	113	84	25	9	4	A2
24	1/28/2014	22:23:39	38.3927	20.4418	2.22E+22	4.2	15.9	12	22	60	175	115	86	30	13	4	B1
25	1/30/2014	11:06:18	38.4050	20.5267	4.06E+22	4.4	9.2	8	4	73	159	100	70	18	12	4	C1
26	1/31/2014	6:52:47	38.4210	20.4843	4.06E+22	4.4	12.4	12	19	64	170	113	81	26	7	4	B1
27	1/31/2014	12:45:40	38.4180	20.4677	2.96E+22	4.3	18.6	13	18	65	170	112	81	25	12	4	A1
28	2/1/2014	16:33:38	38.1727	20.3876	7.35E+22	4.5	10.6	12	17	68	175	109	85	22	8	4	B1
29	3/2/2014	3:08:44	38.2527	20.3948	2.46E+24	6.0	10.5	17	20	67	174	112	84	23	10	5	A1
30	2/4/2014	19:42:12	38.2817	20.3702	2.22E+22	4.2	16.5	11	23	66	172	116	83	24	10	4	B1
31	2/7/2014	3:26:43	38.3253	20.4325	2.22E+22	4.2	13.0	9	25	60	170	120	81	30	12	4	A2

Preprints (www.preprints.org) | NOT PEER-REVIEWED | Posted: 4 September 2020 doi:10.20944/preprints202009.0080.v1

32	2/7/2014	8:59:43	38.2338	20.4558	2.22E+22	4.2	12.9	12	20	65	175	114	81	25	9	4	B1
33	2/9/2014	8:22:58	38.1752	20.3675	7.35E+22	4.5	11.2	12	20	67	180	110	90	23	12	4	B1
34	2/12/2014	10:34:31	38.1655	20.3538	8.17E+22	4.6	11.1	12	25	70	166	120	77	21	14	5	B1
35	2/14/2014	3:38:33	38.1677	20.3432	8.17E+22	4.7	9.8	13	20	67	170	114	81	23	13	5	B1
36	2/21/2014	15:18:23	38.2147	20.9720	7.35E+22	4.5	16.2	13	26	73	177	117	87	17	10	4	B1
37	3/5/2014	12:49:20	38.0780	20.3092	8.17E+22	4.6	20.4	12	30	70	170	123	80	15	12	4	A1
38	3/5/2014	15:08:43	38.0792	20.3467	1.38E+22	4.1	18.0	14	18	70	168	112	79	20	13	4	B1
39	3/5/2014	18:42:02	38.1423	20.4185	9.52E+21	4.0	16.3	12	22	65	168	117	79	25	10	4	B1
40	3/10/2014	23:27:48	38.2087	20.2852	9.52E+21	4.0	13.4	12	25	70	170	120	85	26	9	4	B1
41	11/5/2014	14:22:24	38.1027	20.4877	1.38E+22	4.1	16.6	10	23	68	175	115	85	22	8	4	A1
42	11/7/2014	7:41:38	38.1020	20.4358	8.17E+22	4.7	17.7	9	20	64	170	114	81	26	9	4	B1
43	11/8/2014	23:15:42	38.0998	20.4400	4.065E+25	5.0	18.4	11	22	67	168	117	79	23	10	5	C1
44	11/12/2014	6:31:37	38.2893	20.4722	9.52E+21	4.0	13.8	9	19	62	170	114	81	28	8	4	B1
45	11/13/2014	9:37:53	38.3803	20.5142	2.96E+22	4.3	12.4	13	23	60	172	117	83	30	7	4	A1
46	11/24/2014	7:20:32	38.3022	20.3630	1.38E+22	4.1	15.2	13	17	68	175	109	85	22	12	4	B1
47	12/11/2014	22:24:22	38.3815	20.4412	8.17E+22	4.6	28.0	12	25	60	170	120	81	30	8	4	B1
48	3/31/2015	15:48:41	38.3173	20.5220	8.17E+22	4.6	11.3	14	18	64	170	112	81	26	13	4	A2
49	4/4/2015	4:38:19	38.3108	20.5308	4.06E+22	4.4	13.4	12	19	62	170	114	81	28	10	4	B1
50	6/2/2015	14:04:21	38.1465	20.4722	4.06E+22	4.4	15.3	12	20	69	169	114	80	21	9	5	A1
51	11/17/2015	11:49:45	38.4862	20.4857	9.52E+21	4.0	7.5	13	22	70	168	116	79	20	7	5	A2
52	11/18/2015	5:18:13	38.4967	20.5177	4.06E+22	4.4	13.6	12	20	77	173	112	83	13	8	5	B1
53	11/19/2015	17:45:55	38.4623	20.4952	2.96E+22	4.3	12.5	8	40	68	176	132	86	22	9	4	B1
54	11/20/2015	5:12:24	38.4703	20.4875	8.17E+22	4.7	12.4	14	20	64	178	111	88	26	12	4	A1
55	1/4/2016	7:21:45	38.3155	20.4012	2.96E+22	4.3	15.0	13	20	88	166	111	76	2	12	4	A2
56	4/11/2016	18:53:44	38.2133	20.3325	1.38E+22	4.1	20.5	12	15	87	144	107	54	4	13	4	A1
57	15/01/2019	1:11:49	38.2898	20.4142	2.22E+22	4.2	11.2	11	4	73	159	100	70	18	8	4	A1

Table A2. Source Parameters of the main events as well as for the intermediate magnitudes for Lefkas Seismic Sequence for the period 2015 – 2019. Nr is the event number. Lat and Lon are the geographical coordinates of each event, as they calculated by National Observatory of Athens; M_0 is the seismic moment in dyn*cm, M_w is the moment magnitude; Strike, Dip, Rake of the two nodal planes is the seismic parameters as they calculated from the inversion; CLVD is the percentage of Compensated Linear Vector Dipole which describes seismic sources with no volume changes; Nr of stations is the number of stations used in inversion and finally the quality of the solution depending from the Misfit and the percentage CLVD

N_r	Origin		Location		M_0 (dyn*cm)	M_w	Depth (km)		Plane 1			Plane 2			CLVD (%)	Nr of stations	Quality
	Date	Time	Lat (°)	Lon (°)			Catalog	MT	Strike (°)	Dip (°)	Rake (°)	Strike (°)	Dip (°)	Rake (°)			
1	11/17/2015	7:10:07	38.6655	20.6002	4.402E+28	6.4	10.7	10	290	88	-12	20	82	-178	15	6	A1
2	11/17/2015	8:33:40	38.6515	20.5570	4.065E+25	5.0	8.7	8	112	87	6	22	84	177	8	6	A1
3	11/17/2015	11:49:45	38.4862	20.4857	1.439E+22	4.0	7.5	2	310	25	-8	43	83	-123	10	4	B1
4	11/17/2015	11:57:25	38.7025	20.6145	6.133E+22	4.5	9.9	4	24	65	172	117	83	25	12	5	A2
5	11/17/2015	12:37:56	38.7022	20.6538	1.300E+23	4.7	4.8	4	144	89	14	53	76	179	7	4	A1
6	11/17/2015	19:39:34	38.7040	20.6017	2.240E+22	4.2	8.5	4	308	85	4	41	86	-175	10	4	A1
7	11/18/2015	5:18:13	38.4967	20.5177	5.817E+22	4.4	13.6	8	336	86	172	67	81	9	9	5	A2
8	11/18/2015	12:15:38	38.8443	20.5915	3.857E+23	5.0	17.2	10	203	71	-174	111	84	-19	6	5	A1
9	11/18/2015	13:03:14	38.7197	20.6288	1.483E+23	4.7	8.3	4	314	96	-24	53	67	-158	5	5	A1
10	11/18/2015	18:30:07	38.7238	20.6280	2.443E+22	4.2	6.3	2	290	86	155	21	59	7	10	4	A2
11	11/20/2015	5:12:24	38.4703	20.4875	1.746E+23	4.8	12.4	8	116	80	5	26	85	170	6	5	A1
12	11/20/2015	9:33:14	38.6347	20.5830	7.662E+22	4.5	10.7	6	203	80	175	294	85	10	7	5	A1
13	11/20/2015	23:37:04	38.7128	20.6093	9.104E+25	4.6	12.0	2	302	57	-10	37	81	-146	9	4	A1
14	11/21/2015	0:41:56	38.7148	20.6170	7.199E+22	4.5	9.3	2	297	80	-20	31	69	-168	10	4	A1
15	1/4/2016	18:00:55	38.6037	20.5917	2.72E+22	4.2	14.1	10	29	47	-174	295	86	-43	10	4	A2
16	12/25/2017	23:47:05	38.5937	20.5613	5.817E+22	4.4	4.7	8	111	70	50	357	52	150	7	4	A1
17	1/15/2019	1:25:05	38.9428	20.6178	5.817E+22	4.4	18.8	11	119	58	30	14	71	150	5	4	A1
18	2/5/2019	2:26:09	38.9803	20.5870	4.065E+25	5.0	13.2	10	224	27	170	317	85	54	6	5	A1
19	43522	10:05:59	38.8623	20.6104	1.439E+22	4.0	4.6	8	291	53	-9	27	83	-142	10	4	A1

Table A3. Source Parameters of the main events as well as for the intermediate magnitudes for Zande Seismic Sequence for the period 2018 – 2019. Nr is the event number. Lat and Lon are the

Preprints (www.preprints.org) | NOT PEER-REVIEWED | Posted: 4 September 2020 doi:10.20944/preprints202009.0080.v1

geographical coordinates of each event, as they calculated by National Observatory of Athens; M_0 is the seismic moment in dyn*cm, Mw is the moment magnitude; Strike, Dip, Rake of the two nodal planes is the seismic parameters as they calculated from the inversion; CLVD is the percentage of Compensated Linear Vector Dipole which describes seismic sources with no volume changes; Nr of stations is the number of stations used in inversion and finally the quality of the solution depending from the Misfit and the percentage CLVD.

Nr	Origin		Location		M_0 (dyn*cm)	M_w	Depth (km)		Plane 1			Plane 2			CLVD (%)	Nr of stations	Quality
	Date	Time	Lat (°)	Lon (°)			Catalog	MT	Strike (°)	Dip (°)	Rake (°)	Strike (°)	Dip (°)	Rake (°)			
1	10/25/2018	22:22:53	37.3482	20.5547	1.746E+23	4.8	5.0	15	140	70	80	347	22	116	10	4	A1
2	10/25/2018	22:54:50	37.3516	20.4922	1.45E+26	6.7	12.8	17	123	42	30	10	70	128	20	5	A2
3	10/26/2018	5:48:36	37.3592	20.5058	4.065E+25	5.0	3.1	16	19	39	139	143	66	59	12	5	A1
4	10/26/2018	1:06:03	37.3887	20.8560	7.35E+22	4.5	5.6	15	33	47	170	130	83	43	15	4	A2
5	10/26/2018	0:13:39	37.4660	20.6712	7.35E+22	4.5	5.7	18	19	28	176	113	88	62	13	4	A1
6	10/26/2018	12:41:13	37.3753	20.5360	5.42E+22	5.1	7.3	19	23	28	163	128	82	63	8	4	A1
7	10/26/2018	16:07:09	37.4248	20.5892	4.06E+22	4.4	6.7	15	341	56	140	69	57	41	10	5	A2
8	10/27/2018	5:28:46	37.4743	20.6392	4.06E+22	4.4	5.1	12	25	61	126	149	45	44	12	4	A1
9	10/30/2018	2:59:59	37.5938	20.5123	5.82E+24	5.4	6.9	18	36	41	152	148	72	53	7	4	A1
10	10/30/2018	8:32:26	37.4840	20.4300	1.746E+23	4.8	11.3	17	124	81	77	360	16	145	10	5	A1
11	10/30/2018	15:12:02	37.4575	20.4522	1.90E+23	5.8	5.5	19	18	28	164	122	83	63	5	5	A1
12	11/1/2018	2:44:48	37.3673	20.5658	8.17E+22	4.6	11.3	18	20	25	166	123	84	66	13	4	A1
13	11/4/2018	3:12:44	37.3785	20.4113	1.746E+23	4.8	5.2	17	16	28	166	119	84	66	9	5	A1
14	11/5/2018	6:46:12	37.6268	20.4863	7.35E+22	4.5	8.3	17	10	24	179	101	90	66	10	4	A1
15	11/11/2018	23:38:35	37.6327	20.5055	1.746E+23	4.8	7.0	18	12	27	178	104	89	63	12	5	A1
16	11/15/2018	9:02:05	37.5227	20.6825	1.746E+23	4.8	17.4	15	22	29	156	133	79	63	12	5	A1
17	11/15/2018	9:09:26	37.4887	20.6503	7.35E+22	4.5	6.8	17	42	49	167	141	80	42	10	4	A2
18	12/25/2018	1:41:27	37.3243	20.7963	8.17E+22	4.6	12.3	14	14	25	168	115	85	66	10	4	A2

References:

1. Lekkas E.; Danamos G.; Mavrikas G. Geological structure and evolution of the islands of Kefalonia Ithace, Bulletin of Geological Society of Greece, 2001.

2. Stiros, S.C.; Pirazzoli, P.A.; Laborel, J.; Laborel-Deguen, F. The 1953 earthquake in Cephalonia (Western Hellenic Arc): coastal uplift and halotectonic faulting. *Geophys. J. Int*., **1994**; *Volume 117 (3)*, pp. 834–849.

3. Louvari E.; Kiratzi AA.; Papazachos BC. The Cephalonia transform fault and its extension to western Lefkas Island (Greece). *Tectonophysics* **1999**, *Volume 308:223-36*.

4. Finetti, I.; Morreli, C. Geophysical exprolation of the Mediterranean sea. Boll. Geofis. Teor., 1973 Appl., 15, 263-341.

5. Stride, A.; Belderson, R.; Kenyon, N. Evolving miogeoanticlines of the Eastern Mediterranean (Hellenic, Calabrian and Cyprus outer ridges). Philos. Trans. R. Soc. London, 282, 255-285, 1979.

6. Finetti, I. Structure, stratigraphy and evolution of central Mediterranean. Boll. Geofis. Teor. Appl., 24, 247-426, 1982

7. BP Co. 1971. The geological results of petroleum exploration in western Greece.

8. Mercier, J.; Bousquet, B.; Delibassis, N.; Drakopoulos, I.; Keraudren, B.; Lemeille, F.; Sorel, D. 1972. Deformations en compression dans le Quaternaire des rivages ionien, Donnes neotectoniques et seismiques. C. R. Ac. Sc. Paris, 1972, 275, 2307 -10.

9. Cushing, M. Evolution structural de la marge nord-ouest hellenique dans l"ile de Lefkas et ses environs (Grece nord-occidentale). PhdThesis, Univ. d" Orsay, 1985.

10. Scordilis, E.M.; Karakaisis, G.F.; Karakostas, B.G.; Panagiotopoulos, D.G.; Comninakis, P.E.; Papazachos, B.C. Evidence for transform faulting in the Ionian sea: The Cephalonia island earthquake sequence of 1983. *PureAppl. Geophys*, **1985**, *Volume 123*, 388-397.

11. Anderson, H., Jackson, J. Active tectonics of the Adriatic region. *Geophys. J.R. Astr. Soc*., **1987**, *Volume 91*, p.p. 937-983.

12. James Jackson and Dan McKenzie, The relationship between plate motions and seismic moment tensors, and the rates of active deformation in the Mediterranean and Middle East, *Geophysical Journal* **1988** *Volume 93*, p.p. 45-73

13. Kiratzi, A. A; Langston C.A. Moment tensor inversion of the 1983 January 17 Kefallinia event of Ionian Islands (Greece), *Geophysical Journal International* **1991**; *Vol.105* Issue 2; pp. 529 – 535.

14. Hatzfeld, D.; Kassaras, I.; Panagiotopoulos, D.; Amorese, D.; Makropoulos, K.; Karakaisis, D.; Coutant, O. Microseismicity and strain pattern in northwestern Greece. *Tectonics*, **1995**, *Volume 14*, No 4, pp. 773-785.

15. Kahle, H;, Muller, M.; Geiger, A.; Danuser, G.; Mueller, S.; Veis, G.; Billiris, H.; Paradissis, D. 1995. The strain field in northwestern Greece and the Ionian islands: results inferres from GPS measurements. *Tectonophysics*, **1995**, *Volume 249*, pp. 41-52

16. Kahle, H.; Muller, M.; Veis, G. 1996. Trajectories of crustal deformation of Western Greece fromGPS observations 1989 -1994. *J. Geophys. Lett*., **1996**, *Volume 23*, pp. 677-680.

17. Makropoulos, K.; Diagourtas, D.; Kassaras, J.; Kouskouna, V.; Papadimitriou, P.; Ziazia, M. The November - December 1994 Lefkas (W. Greece) earthquake sequence: results from in situ seismological survey (abstract). 1stCongress of the Balkan Geophysical Society, Sept. 23-27, Athens, 1996.

18. Sachpazi M., Hirn A., Clément Ch., Laigle M., Haslinger F., Kissling E., Charvis Ph., Hello Y., Lépine J. C., Sapin M., and Ansorge J. Western Hellenic subduction and Cephalonia Transform: local earthquakes and plate transport and strain. *Tectonophysics*, **2000**, *Volume 319*, pp. 301-319.

19. Konstantaras, A. Expert knowledge-based algorithm for the dynamic discrimination of interactive natural clusters. *Earth Science Informatics* **2016**, *Volume 9*, pp. 95-100.

20. Konstantaras, A. Classification of distinct seismic regions and regional temporal modelling of seismicity in the vicinity of the Hellenic seismic arc. IEEE *Journal of Selected Topics in Applied Earth Observations and Remote Sensing* **2013**, *Volume 6(4)*, pp. 1857-1863.

21. Konstantaras, A.; Vallianatos, F.; Varley, M.R.; Makris, J.P. Soft-computing modelling of seismicity in the southern Hellenic Arc. *IEEE Geoscience & Remote Sensing Letters* **2008**; *Volume 5(3)*, pp. 323-327.

22. Moshou, A. Strong earthquake sequences in Greece during 2008-2014: Moment Tensor inversions and fault plane discrimination. *Open Journal of Earthquake Research* **2020**, *Volume 9*, pp. 323-348.

23. Randal, G.E. Efficient calculation of complete differential seismograms for laterally homogeneous earth models. *Geophysical Journal International* **1994**, *Volume 118*, pp.245 – 254.

24. Kennett, B. N.L. Seismic wave propagation in Stratified Media, Cambridge: Cambridge University Press, 1983.

25. Haslinger, F.; Kissling, E.; Ansorge, J.; Hatzfeld, D.; Papadimitriou, E.; Karakostas, V.; Makropoulos, K.; Kahl, H – G.; Peter.Y. 3D crustal structure from local earthquake tomography around the Gulf of Arta (Ionian region, NW Greece). *Tectonophysics* **1999**, *Volume 304*, pp. 201–218.

26. Melis, N.; Konstantinou, K,; Real-time Seismic Monitoring in the Greek Region: An Example from the 17 October 2005 East Aegean Sea Earthquake Sequence. *Seismological Research Letters* **2006**, *Volume 77*, pp. 364 – 370.

27. Konstantinou, K.; Melis, N.; Boukouras, K. Routine Regional Moment Tensor Inversion for Earthquakes in the Greek Region: The National Observatory of Athens (NOA) Database (2001 – 2006), *Seismological Research Letters* **2010**, *Volume 81*, Number 5, pp. 750 – 760.

28. Sachpazi, M.; Hirn, A.; Clement, C.; Haslinger, F.; Kissling, E.; Charvis, P. Western Hellenic subduction and Cephalonia Transform: local earthquakes and plate transport and strain *Tectonophysics*,**1998**, *Volume 319*; pp. 301 – 319.

29. Axaridou, A.; Chrysakis, I.; Georgis, C.; Theodoridou, M.; Doerr, M.; Konstantaras, A.; Maravelakis, E. 3D-SYSTEK: Recording and exploiting the production workflow of 3D-models in cultural heritage. The 5th International Conference on Information, Intelligence, Systems & Applications (IISA 2014), 2014; pp. 51-56

30. Maravelakis, E.; Konstantaras, A.; Kabassi, K.; Chrysakis, I.; Georgis, C.; Axaridou, A. 3DSYSTEK web-based point cloud viewer. The 5th International Conference on Information, Intelligence, Systems & Applications (IISA 2014), 2014; pp. 262-266.

31. Bouckovalas G. Information about the EARTHQUAKES OF KEFALONIA 26/1 and 3/2/2014, National Technical University of Athens, 2014.

32. Papathanassiou, G., Ganas, A., Moshou, A., & Valkaniotis, S. Geoenviromental effects of the M=6.4 17 November 2015 earthquake on south Lefkas, Ionian Sea, Greece. Bulletin of the Geological Society of Greece, 2016, Volume 50(1), pp. 521-539.

33. Papadopoulos, G. A.; Karastathis, V. K.; Ganas, A.; Pavlides, S.; Fokaefs, A.; Orfanogiannaki, K. The Lefkas, Ionian Sea (Greece), shock (Mw 6.2) of 14 August 2003: Evidence for the characteristic earthquake from seismicity and ground failures. *Earth Planet. Space*, **2003**; *Volume 55;* pp. 713–718.

34. Karakostas, V.; Papadimitriou, E.; Papazachos, C. Properties of the 2003 Lefkas, Ionian islands, Greece, Earthquake seismic sequence and seismicity triggering. *BSSA*; **2003** *Volume 94*/5; pp. 1976-1981.

35. Benetatos C, Kiratzi A, Roumelioti Z, et al. The 14 August 2003 Lefkas Island (Greece) earthquake: Focal mechanisms of the mainshock and of the aftershock sequence. *J Seismol*, **2005**; *Volume 9*:171-90.

36. Papathanassiou, G.; Pavlides, Sp.; Ganas, A. The 2003 Lefkas earthquake: Field observations and preliminary microzonation map based on liquefaction potential index for the town of Lefkas, *Engineering Geology*, **2003**; *Volume 82*, Issue 1, pp. 12-31.

37. Ganas, A.; Briole, P.; Papathanassiou, G.; Bozionelos, G.; Avallone, A,; Melgar, D.; Argyrakis, P.; Valkaniotis, S.; Mendonidis, E.; Moshou, A.; Elias, P. A preliminary report on the Nov 17, 2015 M= 6.4 South Lefkas earthquake, Ionian Sea, Greece. Report on emsc – csem, https://www.emsc-csem.org/Doc/Additional_Earthquake_Report/470390/Lefkas%2017%20Nov%202015%20earthquake%20report.pdf

38. Sokos, E., Gallovič, F., Evangelidis, C.P., Serpetsidaki, A., Plicka, V., Kostelecký, J., Zahradník, J. The 2018 Mw 6.8 Zande, Greece, earthquake: dominant strike-slip faulting near subducting slab. *Seismol. Res. Lett. XX*, **2020**, 1–12. https://doi.org/10.1785/0220190169

39. Zahradnik, J., Sokos, E., Plicka, V., 2018. Zande 25/10/2018, Mw 6.8 Earthquake: Superposition of Strike-Slip and Thrust? EMSC Web Report, https://www.emsccsem.org/Files/news/Earthquakes_reports/Zande_2018_Report.pdf

40. Ganas, A., Briole, P., Bozionelos, G., Elias, P., Valkaniotis, S., Tsironi, V., Moshou, A., Andritsou, N. The October 25, 2018 M6.7 Zande Earthquake Sequence (Ionian Sea, Greece): Fault Modelling from Seismic and GNSS Data and Implications for Seismic Strain Release Along the Western Hellenic Arc. Bull. Geological Society of Greece, 2019, Special Publication 7, pp. 602–603.

41. Chousianitis, K., & Konca, A. O. Intraslab deformation and rupture of the entire subducting crust during the 25 October 2018 Mw 6.8 Zande earthquake. *Geophysical Research Letters*, **2019**, *Volume 46*. https://doi.org/10.1029/2019GL085845

42. Papadimitriou, P.; Chousianitis, K.; Agalos, A.; Moshou, A.; Lagios, E.; Makropoulos, K. The spatially extended 2006 April Zande (Ionian Islands, Greece) seismic sequence and evidence for stress transfer. *Geophys. J. Int*. **2012**, *Volume 190* (2) pp. 1025 – 1040.

43. Estey, L. H.; Meertens,C.M.TEQC: The Multi-Purpose Toolkit for GPS/GLONASS Data, GPS Solutions (pub. by John Wiley & Sons) **1999**. *Volume 3*, No. 1, pp. 42-49.

44. Bertiger, W.; Desai, S.; Haines, B.; Harvey, N.; Moore, A.; Owen, S.; Weiss, J. Single receiver phase ambiguity resolution with GPS data; *J. Geodesy* **2010**, *Volume 84*(5); pp. 327-337.

45. Zumberge, J. F.; Heflin,M.B.; Jefferson, D.C.; Watkins, M.M; Webb, F.H. Precise point positioning for the efficient and robust analysis of GPS data from large network. *J. Geophys. Res*., **1997**; *Volume 102* (B3), pp. 5005-5017.

46. Hill, E. M.; Blewitt, G. Testing for fault activity at Yucca Mountain, Nevada, using independent GPS results from ths BARGEN network; *Geophys. Res. Lett*, **2006**, *Volume 33*.

47. Rozsa, S. Modelling Tropospheric Delays Using the Global Surface Meteorological Parameter Model GPT2; *Periodica Polytechnica Civil Engineering*, **2014**, *Volume 58* (4), pp.310-308.

48. Wang M, Li B. Evaluation of Empirical Tropospheric Models Using Satellite-Tracking Tropospheric Wet Delays with Water Vapor Radiometer at Tongji, China. Sensors (Basel). **2016**, *Volume 16(2):*186. Published 2016 Feb 2. doi:10.3390/s16020186.

49. Steigenberger P.; Boehm J.; Tesmer V. Comparison of GMF/GPT with VMF1/ECMWF and Implications for Atmospheric Loading, Journal of Geodesy, 2009; DOI: 10.1007/s00190-009-0311-8 .

50. Wahr, J. M. Deformation induced by polar motion, *J. Geophys. Res*. **1995**. *Volume 90*(B11); pp. 9363–9368, doi:10.1029/JB090iB11p09363

51. A. Roy.1, M. Matos.2, K. J. Marfurt, (2010), "Automatic Seismic Facies Classification with Kohonen Self Organizing Maps - a Tutorial", Geohorizons, Dec 2010 pp.6-14.

52. B. Sick, M. Guggenmos, M. Joswig, (2015), "Chances and limits of single-station seismic event clustering by unsupervised pattern recognition", *Geophys. J. Int*. **2015**, *Volume 201*, 1801–1813.

53. Shang, X., Li, X., Morales-Esteban, A., Asencio-Cortés, G., Wang, Z. "Data Field-Based K-Means Clustering for Spatio-Temporal Seismicity Analysis and Hazard Assessment", *MDPI, Remote Sens*. **2018**, *Volume 10*, 461; doi:10.3390/rs10030461

54. Sakkas, V.; Lagios, E. Ground deformation effects from the ~M6 earthquakes (2014–2015) on Cephalonia–Ithaca Islands (Western Greece) deduced by GPS observations. *Acta Geophysica*, **2017**. *Volume 65(1),* pp.207-222.

55. Ganas, A.; Cannavo, F.; Chousianitis, K.; Kassaras, I.; Drakatos, G. Displacements recorded on continuous GPS stations following the 2014 M6 Cephalonia (Greece) earthquakes: dynamic characteristics and kinematic implications. *Acta Geodyn. Geomater*, **2015**, *Volume 12 (1),* 5–https://doi.org/10.13168/AGG.2015.0005. 177

56. Papadopoulos, G.; Karastathis, V.; Koukouvelas, I.; Sachpazi, M.; Baskoutas, I.; Chouliaras, G.; Agalos, A.; Daskalaki, E.; Minadakis, G.; Moschou, A.; Mouzakiotis, A.; Orfanogiannaki, K.; Papageorgiou, A.; Spanos,D.; Triantafyllou, I. The Cephalonia, Ionian Sea (Greece), sequence of strong earthquakes of January-February 2014: a first report. *Research in Geophysics*, **2014**; *Volume 4*, p.p. 19 – 30.

57. Karastathis V, Koukouvelas I, Ganas A, et al. The strong Mw6 earthquake of 26th January 2014 in Cephalonia island, Ionian Sea, Greece: a first report. Geophys. Res. Abstr. 2014, 16: EGU 2014-1700, Europ. Geosci. Union General Assembly, 2014.